

# UC San Diego

## UC San Diego Electronic Theses and Dissertations

### Title

Quantum Algorithms for Searching Manifolds

### Permalink

<https://escholarship.org/uc/item/4934z45v>

### Author

Sherkat-Massoom, Hooman

### Publication Date

2018

Peer reviewed|Thesis/dissertation

UNIVERSITY OF CALIFORNIA, SAN DIEGO

**Quantum Algorithms for Searching Manifolds**

A dissertation submitted in partial satisfaction of the  
requirements for the degree  
Doctor of Philosophy

in

Mathematics

by

Hooman Sherkat-Massoom

Committee in charge:

Professor David A. Meyer, Chair  
Professor Craig Callendar  
Professor Michael Holst  
Professor Kenneth Intriligator  
Professor Justin Roberts

2018

Copyright  
Hooman Sherkat-Massoom, 2018  
All rights reserved.

The dissertation of Hooman Sherkat-Massoom is approved, and it is acceptable in quality and form for publication on microfilm and electronically:

---

---

---

---

---

---

Chair

University of California, San Diego

2018

## EPIGRAPH

*Truth in drama is forever elusive. You never quite find it, but the search for it is compulsive. The search is clearly what drives the endeavour. The search is your task.*

— Harold Pinter

## TABLE OF CONTENTS

Signature Page . . . . .		iii
Epigraph . . . . .		iv
Table of Contents . . . . .		v
List of Figures . . . . .		vii
List of Tables . . . . .		viii
Acknowledgements . . . . .		ix
Vita . . . . .		x
Abstract of the Dissertation . . . . .		xi
Chapter 1	Introduction . . . . .	1
	1.1 Quantum Computing . . . . .	1
	1.2 Grover’s Algorithm . . . . .	4
	1.3 Analog Search Algorithms . . . . .	5
	1.4 Spatial Search . . . . .	7
Chapter 2	Continuous Quantum Spatial Search . . . . .	10
	2.1 Search Phase . . . . .	14
	2.2 Check Phase . . . . .	18
Chapter 3	Quantum Search on $S^1$ . . . . .	30
	3.1 Search Phase . . . . .	30
	3.2 Check Phase . . . . .	34
	3.3 Analytic Results . . . . .	41
	3.4 Numerical Results . . . . .	45
Chapter 4	Quantum Search on $T^2$ . . . . .	50
	4.1 Self-adjoint Extensions . . . . .	50
	4.2 Delta Potentials in 2D . . . . .	52
	4.3 Search Phase . . . . .	55
	4.4 Check Phase . . . . .	57
	4.5 Analytic Results . . . . .	61
Appendix A	Square-root Measurement in the Continuum . . . . .	67
	A.1 Quantum State Discrimination . . . . .	67
	A.2 SRM for a Geometrically Uniform Ensemble on a Torus . . . . .	68

Bibliography . . . . . 74

## LIST OF FIGURES

Figure 2.1: If we do $R = 4$ checks with overlapping intervals, no point in the original interval will be further than $r = \epsilon/8$ from the center of one of the overlapping intervals . . . . .	24
Figure 3.1: Quantization condition for unbound states . . . . .	33
Figure 3.2: Quantization condition for the bound state . . . . .	33
Figure 3.3: Comparing the first three eigenstates for a particle on a circle with (second column) and without (first column) a delta potential. The the second and third plots of first column actually show a linear combination of eigenstates for the energies $E_1$ and $E_2$ , which are degenerate with multiplicity 2. . . . .	35
Figure 3.4: Quantization condition for the unbound and bound states for different values of $\gamma_c$ ; the first row satisfies $\gamma_c < w(L - w)/L$ , while the second does not. . . . .	38
Figure 3.5: The first two eigenstates for a particle in a box without (first row) and with a delta potential (second and third rows). The second and third rows have different values of $\gamma_c$ ; the third row satisfies the condition so that the ground state is a bound state. . . . .	39
Figure 3.6: A plot of the detuning $\Delta$ as a function of what proportion of the way into the box $w$ is, for three different values of $\gamma_c$ . Note that $\Delta$ grows as $w$ approaches the center of the box, and this effect is stronger for smaller $\gamma_c$ . . . . .	40
Figure 3.7: Scaling $\gamma_c$ and $\epsilon$ by the same factor (in this case, 10) will scale the detuning $\Delta$ by that factor. . . . .	43
Figure 3.8: A list plot of the cost and the best fit of the form $aN^2 \log \delta' N + bN$ . The function was fit on the blue data; it matches the rest of the data (in red) quite well. . . . .	46
Figure 3.9: A list plot of $\gamma_s$ , along with its mean. $\gamma_s$ and $t_s$ are held nearly constant, mimicking the strategy used for the analytic scaling. . . . .	48
Figure 3.10: A list plot of $t_s$ , along with its mean. $t_s$ and $\gamma_s$ are held nearly constant, mimicking the strategy used for the analytic scaling. . . . .	48
Figure 3.11: A list plot of $t_c$ , along with the line of best fit. $t_c$ grows nearly linearly, mimicking the strategy used for the analytic scaling. . . . .	49
Figure 3.12: A list plot of $p_1$ , along with its mean. It is nearly constant as a result of $t_c$ growing nearly linearly, mimicking the strategy used for the analytic scaling. . . . .	49



## LIST OF TABLES

Table 1.1: Several important quantum gates. Not listed are the Toffoli gate (controlled CNOT) and the Fredkin gate (controlled SWAP). . .	3
---	---

## ACKNOWLEDGEMENTS

I'd like to thank my advisor, my reseach group, my friends, and my family  
– your support has been invaluable.

VITA

2009                    **B.S. with Highest Honors in Mathematics, UCLA**

2011                    **M.A. in Mathematics, UCSD**

2013                    **C.Phil. in Mathematics, UCSD**

2018                    **Ph.D in Mathematics, UCSD**

ABSTRACT OF THE DISSERTATION

**Quantum Algorithms for Searching Manifolds**

by

Hooman Sherkat-Massoom

Doctor of Philosophy in Mathematics

University of California San Diego, 2018

Professor David A. Meyer, Chair

Quantum computing is a system of computation that exploits the quantum-mechanical nature of reality at nano-scales in order to perform certain operations in a way that can scale better than is possible with classical computing. While the hardware side of quantum computing is still in its infancy, many quantum algorithms - sets of instructions to run on a quantum computer in order to complete particular tasks - have been designed and analyzed. One of the most famous of these is Grover's algorithm, an algorithm for searching a database. Two types of generalizations of Grover's algorithm have been studied: spatial search algorithms

(algorithms for searching discrete spaces) and “analog” search algorithms (algorithms performed by the evolution of physical systems). We develop and analyze algorithms that are generalizations of both those generalizations – an analog search algorithm for searching continuous, rather than discrete, spaces.

# Chapter 1

## Introduction

In this chapter, we begin by giving a basic introduction to quantum computing. We then describe Grover's algorithm, one of the first quantum algorithms. We conclude with a brief overview of two generalizations of Grover's algorithm.

### 1.1 Quantum Computing

Computation is the processing of information by algorithms – a well-defined step-by-step process for taking an input and transforming it into an output. Classical computation is the processing of classical information (roughly, that which describes the state of a system which behaves according to the laws of classical mechanics). The fundamental unit of classical information is the bit, a system which can take on two values; classical information is represented by bit strings.

A bit is most commonly represented as a 0 or 1; a bit string is a binary

string in  $\bigcup_{n \geq 0} \{0, 1\}^n$ . A computation is performed by manipulating an input bit string via a sequence of gates implementing Boolean functions (functions that take in a bit string and output a bit).

Quantum computing, then, is the processing of quantum information. Quantum information is that which describes the state of a quantum system; its fundamental unit is the quantum bit, or qubit. The qubit is a two-level quantum system – a two complex-dimensional Hilbert space commonly represented as  $\mathbb{C}^2$  (to which all two dimensional Hilbert spaces are isomorphic). A qubit string is an element of  $(\mathbb{C}^2)^{\otimes n}$ , for some  $n$ , if we've chosen a basis for each qubit. The properties of quantum systems, such as superposition and entanglement, allow certain computations to be performed more quickly (or, rather, to scale better) than is possible classically.

In the quantum gate model, a quantum algorithm consists of the preparation of an input qubit string, the transformation of it via a sequence of quantum gates, and, finally, the measurement of the string. Quantum gates are maps that implement unitary transformations. As quantum measurements are random processes, many quantum algorithms only succeed with high probability, though some do succeed with probability 1. Many algorithms exploit quantum phenomena such as superposition and entanglement to carefully cancel out the “wrong answers” and increase the probability the desired output is measured.

If we are working with  $n$  qubits, we have a  $2^n =: N$  dimensional system with basis  $\{|b_1\rangle \dots |b_n\rangle \mid b_i \in \{0, 1\}\}$ . We can relabel the basis as  $|0\rangle, |1\rangle, \dots, |N-1\rangle$

by associating  $|i\rangle$  with the binary representation of  $i$  as a bit string. With this, we have an ordered basis, allowing us to represent quantum gates as  $N \times N$  matrices when needed. The table 1.1 lists many common (and crucial) quantum gates, along with their matrix forms.

More on quantum computing and quantum information can be found in the textbooks by Nielsen and Chuang [NC11] or by Rieffel and Polak [RP11].

Table 1.1: Several important quantum gates. Not listed are the Toffoli gate (controlled CNOT) and the Fredkin gate (controlled SWAP).

Symbol	Name	Matrix form
$X$	Pauli-X	$\begin{bmatrix} 0 & 1 \\ 1 & 0 \end{bmatrix}$
$Y$	Pauli-Y	$\begin{bmatrix} 0 & -i \\ i & 0 \end{bmatrix}$
$Z$	Pauli-Z	$\begin{bmatrix} 1 & 0 \\ 0 & -1 \end{bmatrix}$
$R_\theta$	Phase shift	$\begin{bmatrix} 1 & 0 \\ 0 & e^{i\theta} \end{bmatrix}$
$H = H_1$	Hadamard	$\frac{1}{\sqrt{2}} \begin{bmatrix} 1 & 1 \\ 1 & -1 \end{bmatrix}$
$H_m = H^{\otimes m}$	Hadamard	$\frac{1}{\sqrt{2}} \begin{bmatrix} H_{m-1} & H_{m-1} \\ H_{m-1} & -H_{m-1} \end{bmatrix}$
CNOT	Controlled NOT	$\begin{bmatrix} 1 & 0 & 0 & 0 \\ 0 & 1 & 0 & 0 \\ 0 & 0 & 0 & 1 \\ 0 & 0 & 1 & 0 \end{bmatrix}$
$C(Q)$	Controlled Q	$\begin{bmatrix} 1 & 0 & 0 & 0 \\ 0 & 1 & 0 & 0 \\ 0 & 0 & Q_{1,1} & Q_{1,2} \\ 0 & 0 & Q_{2,1} & Q_{2,2} \end{bmatrix}$
SWAP	Swap	$\begin{bmatrix} 1 & 0 & 0 & 0 \\ 0 & 0 & 1 & 0 \\ 0 & 1 & 0 & 0 \\ 0 & 0 & 0 & 1 \end{bmatrix}$



## 1.2 Grover’s Algorithm

**Challenge.** *Suppose your friend Alice has picked a number  $w$  from 1 to  $N$ . She challenges you to guess  $w$  with as few as possible (and nothing but) questions of the form “Is it the number  $m$ ?” What is your best strategy? How well can you do?*

This is the problem of unstructured search. The unstructured nature of the problem means that we may not do anything “clever” (like binary search) that depends on the structure of the set of possible answers. Classically, the problem is  $\Theta(N)$  – we’re certain to find  $n$  in no more than  $N - 1$  guesses, and require  $N/2$  on average. The cost or complexity here is the query complexity: the number of times we must make a query to a black box or oracle (or, in our case, our friend).

Grover’s algorithm [Gro96] is one of the earliest and most famous quantum algorithms. It is a quantum algorithm for solving the unstructured search problem that finds a solution in  $O(\sqrt{N})$  queries – a quadratic speedup. In fact, this has been shown to be optimal [Zal97].

We’ll show how the algorithm is performed.

The classical oracle can be represented by a delta function  $\delta_w$  which returns a 1 on  $w$  and 0 otherwise. The quantum oracle must be invertible (as it is unitary), so it can’t be represented the same way as the classical oracle; it can be made reversible with the help of an ancillary qubit where we record its output. The quantum oracle acts on basis elements as  $|x\rangle |i\rangle \mapsto |x\rangle |i + \delta_w(x)\rangle$ , where the addition is performed mod 2. Note that if the ancilla register is set to  $|-\rangle = \frac{1}{\sqrt{2}}(|0\rangle - |1\rangle)$ , a sin-

gle call to the oracle will perform  $|x\rangle|-\rangle \mapsto (-1)^{\delta_w(x)}|x\rangle|-\rangle$ . We can ignore the ancilla register and just think of the oracle as implementing  $U_w = |x\rangle \mapsto (-1)^{\delta_w(x)}|x\rangle$ .

Let  $U_s = 2|s\rangle\langle s| - I$ , where  $s = \frac{1}{\sqrt{N}}\sum|x\rangle$  is the equal superposition state.

We can now describe Grover's algorithm: initialize the input  $|s\rangle$  (or just initialize in the state  $|0\rangle$  and apply the Hadamard transform  $H_n$ ), then repeat  $U_s U_w$  a certain number of times.  $-U_s$  is the reflection through the hyperplane orthogonal to  $|s\rangle$  and  $U_w = I - 2|w\rangle\langle w|$  is the reflection through the hyperplane orthogonal to  $w$ ; their composition is a rotation in the  $|s\rangle$ - $|w\rangle$  plane. A simple calculation shows that after approximately  $\frac{\pi}{4}\sqrt{N}$  iterations, the state is as close to  $|w\rangle$  as possible. When we measure in the computational basis, we get  $|w\rangle$  with very high probability.

Grover's algorithm can do more than just solve the unstructured search problem. A quantum algorithm for finding the minimum of a function uses a slight generalization of Grover's algorithm as a subroutine [DH96]. More specifically, given an arbitrary function  $f: \{0, \dots, N-1\} \rightarrow \mathbb{Z}$ , it finds the  $x$  mapping to the minimum value of  $f$  using  $O(\sqrt{N})$  evaluations of  $f$ . The  $O(\sqrt{N})$  complexity is a quadratic speedup over the classical solution, as is true of Grover's algorithm for unstructured search.

### 1.3 Analog Search Algorithms

**Challenge.** *Suppose your friend Alice has picked an element  $|w\rangle$  from a given basis of an  $N$ -dimensional Hilbert space. She challenges you to produce the state  $|w\rangle$  as*

*quickly as possible using a Hamiltonian that is a linear combination of  $|w\rangle\langle w|$  and another Hamiltonian independent of  $|w\rangle$ . What is your best strategy? How well can you do?*

This problem, known as the analog analogue to Grover's algorithm, was posed and solved by Farhi and Gutmann [FG98]. That it is an analogue of the unstructured search problem is easy to see – one can convert the unstructured search problem into this problem via the correspondence between the numbers 1 to  $N$  and the basis states  $|1\rangle$  to  $|N\rangle$ . What makes it analog is that, rather than computing using the quantum gate model, the computation is performed through the (continuous time) Hamiltonian evolution of a quantum system.

In fact, the challenge posed was slightly more general:  $|w\rangle$  wasn't chosen from a basis, but was an arbitrary state in the Hilbert space. They then noted that the more specific case was analogous to the Grover problem. We'll present their calculation in the general case, and then specialize at the end.

Suppose we have the Hamiltonian  $H = E|w\rangle\langle w| + E|s\rangle\langle s|$ , where  $|s\rangle$  is just some state in the Hilbert space, not the equal-superposition state (though it will be when we specialize!). We prepare the system in the state  $|s\rangle$  and note that the evolution will stay inside the plane spanned by  $|s\rangle$  and  $|w\rangle$ .

If we let  $x = \langle s|w\rangle$ , then  $|w\rangle$  and  $|r\rangle = \frac{1}{\sqrt{1-x^2}}(|s\rangle - x|w\rangle)$  will be orthogonal

to each other. Computing in the  $|w\rangle, |r\rangle$  basis, it can be shown that

$$\psi(t) = e^{-iEt} \begin{pmatrix} x \cos(Ext) - i \sin(Ext) \\ \sqrt{1-x^2} \cos(Ext) \end{pmatrix}.$$

It follows that the probability of measuring  $\psi$  and getting  $|w\rangle$  is

$$p(t) = \sin^2(Ext) + x^2 \cos^2(Ext),$$

which is equal to 1 at  $t_* = \frac{\pi}{2Ex}$ .

Now we restrict to the case where  $|w\rangle$  has been chosen from the basis  $\{|1\rangle, \dots, |N\rangle\}$  and set  $|s\rangle = \frac{1}{\sqrt{N}} \sum |i\rangle$ . We thus have  $x = \frac{1}{\sqrt{N}}$ , and so  $t_* = \frac{\pi}{2E} \sqrt{N}$ .

We see that the analog analogue's cost has the same scaling as Grover's algorithm.

This is shown to be optimal for this problem in the same paper.

## 1.4 Spatial Search

**Challenge.** *Suppose your friend Alice has picked a vertex  $w$  in an undirected, loopless graph  $G$  with  $N$  vertices. She places a potential  $H_w = -|w\rangle\langle w|$  at  $w$  and challenges you to find  $w$  as quickly as possible using a (quantum) randomly walking particle that evolves according to a multiple of the graph Laplacian  $-L$ . What is your best strategy? How well can you do?*

This new problem is a generalization of the unstructured search problem – namely, as  $G$  can be any simple graph, there is much more structure at play. In the previous challenges, the relationship between  $w$  and another possible answer  $x$

was identical for all  $x \neq w$ . In this case, however, unless  $G$  is the complete graph  $K_N$ ,  $w$  will be adjacent to some vertices but not others. This structure gives rise to the name “spatial search.”

The graphs considered in the spatial search problem are almost always vertex-transitive (so that the choice of  $w$  doesn’t make any difference) and come in an infinite family (so that we can consider the scaling of the cost as  $N$  tends to infinity). This means that there are multiple versions of the challenge, depending on the family of graphs under consideration.

The Laplacian of a graph  $G$  is  $L = A - D$ , where  $A$  is the adjacency matrix of  $G$ , and  $D$  is the diagonal matrix of degrees. We use  $-L$  as the Hamiltonian so that we have a positive-semidefinite operator. The use of the graph Laplacian  $-L$  may seem strange at first, but we’ve actually seen it before: the Grover operator  $U_s = 2|s\rangle\langle s| - I$  used in Grover’s algorithm and the evolution operator  $E|s\rangle\langle s|$  in the analog analogue are equivalent to the Laplacian of the complete graph  $K_N$  (as adding a multiple of the identity to Hamiltonian has no effect on the evolution of the system). The graph Laplacian is in fact a discrete approximation to the Laplace operator  $\Delta$  used in the Schrödinger equation. Thus, a quantum random walk evolving according to the graph Laplacian can be seen as an approximation to the Schrödinger equation on the graph  $G$ , where  $G$  is a discretization of some space. The  $H_w = -|w\rangle\langle w|$  term in the Hamiltonian  $H = -\gamma L - |w\rangle\langle w|$  is an attractive potential marking  $w$ ; it’s the discrete equivalent of a delta potential  $-\delta_w$  at  $w$ .

Search by a quantum random walk can be done either in discrete time or continuous time [Chi10]. In the continuous time version, the  $N$  complex amplitudes given by  $q_j(t) = \langle j | \psi(t) \rangle$  evolve according to the differential equations

$$i \frac{dq_j(t)}{dt} = \sum_k H_{jk} q_k(t).$$

But for the imaginary  $i$  and the  $H$  in place of  $L$ , these are the same equations in a classical continuous time random walk on a graph.

The search algorithm is similar to the analog algorithm: the system is initialized in the state  $|s\rangle = \frac{1}{\sqrt{N}} \sum |i\rangle$ , evolved for some time  $t$ , and then measured. The choice of  $\gamma$  and  $t$  that optimize the success probability is the strategy we seek.

Childs and Goldstone studied this problem [CG04]. Their method involves analyzing the system's energy gap – the difference between the two lowest energy levels of the Hamiltonian – and how much  $|s\rangle$  and  $|w\rangle$  overlap with the two lowest energy eigenstates in order to find the optimal  $\gamma$ . In their paper, they give results for the complete graph  $K_N$ , the  $n$ -dimensional hypercube  $\mathbb{Z}_2^n$  with  $N = 2^n$  vertices, and the  $d$ -dimensional cubic periodic lattice  $\mathbb{Z}_n^d$  with  $N = n^d$  vertices.

For the complete graph and the hypercube,  $t$  is order  $\sqrt{N}$ . For the periodic lattice, the scaling depends on the dimension  $d$ . When  $d \geq 5$ , the full quadratic speedup as achieved, and the algorithm is  $O(\sqrt{N})$ . When  $d = 4$ , the runtime is  $O(\sqrt{N} \log^{3/2} N)$ . Lastly, no speedup is seen for  $d < 4$ : the runtimes are  $O(N)$  for  $d = 3$  and  $O(\frac{N^2}{\log^3(N)})$  for  $d = 2$ . (In fact, numerical results by Wong find that the runtimes are  $O(N)$  for  $d = 1, 2, 3$ . [Won18])

## Chapter 2

# Continuous Quantum Spatial Search

In this chapter we introduce an algorithm for quantum search on a manifold.

**Challenge.** *Suppose your friend Alice has picked her favourite point  $w$  on the manifold  $M$  (by analogy with the finite cardinality of the discrete case,  $M$  has finite volume). She places  $V_w(x)$ , a potential depending on  $w$ , on  $M$ , marking it; the potential can be flipped on and off with a remote. She challenges you to find  $w$  while using the potential for as little time as possible. What is your best strategy? How well can you do?*

Our goal to devise quantum search on manifolds is inspired by the work on search by continuous time quantum walks on graphs – in particular, the results of Childs and Goldstone regarding search on  $d$ -dimensional periodic lattices [CG04].

A  $d$ -dimensional periodic lattice  $\mathbb{Z}_n^d$  can be viewed as an  $N := n^d$ -element discretization of the  $d$ -torus. We are always concerned with the large- $N$  limit scaling of the complexity of search algorithms. In this case, it can be thought of as analyzing the search problem on finer and finer approximations to the  $d$ -torus. It may seem that we could do quantum search on any manifold by performing it on some family of graphs approximating it. This, however, is not that case – in order for us search a manifold, we would need the manifold to have an infinite family of graphs that are all vertex-transitive. This condition is necessary to ensure that our search problem is fair: how long it takes to find the marked point should not depend on which point in particular it is that's been marked (thus, we only consider search on homogeneous  $M$ ). It's a sad fact of life that such families do not exist for all manifolds, even when they are homogeneous: for instance, the sphere  $S^2$  only has the five Platonic solids. Thus, for some manifolds, search cannot be performed on an approximation: it becomes necessary to somehow devise a continuous time, *continuous space* search algorithm.

A second motivating factor comes from those same results: the complexity of search on  $\mathbb{Z}_n^d$  depends on the dimension,  $d$ . In dimensions  $d > 4$ , the full quadratic speedup is achieved, but the complexity is different for dimensions 1 through 4. This dimension dependence is most clear in continuous rather than discrete time algorithms. We hope that perhaps in passing from discrete space to continuous space, there is something else to be learned about search. In particular, when searching on manifolds, the potential effects of geometry – specifically, curvature



– may be revealed.

As in other quantum search algorithms, our aim is to locate a particular marked element  $w$  of a “database.” In this case, however, rather than the database being represented by the complete graph  $K_n$  or some spatial graph, the database is given by a manifold  $M$ . Our search proceeds as analog search algorithms do: to find the point  $w$ , we mark it with a potential, then let a particle “search randomly” by evolving according to a PDE given by the Hamiltonian.

More specifically, the algorithm proceeds in two phases. Let  $w \in M$  be marked by a some potential  $V_w(x)$  depending spatially on  $w$ . During the *search phase*, we let a particle prepared in a uniform distribution (*i.e.*, the equal superposition state) evolve according to the Schrödinger equation for the manifold  $M$ . After letting the particle evolve for some time  $t_s$ , its position is measured. If we have selected  $V_w$  to be an attractive potential, we can hope that the particle will be found near the marked point. In the *check phase*, we look around the measured location and check to see if the marked point is nearby. If it is, we’ve successfully located the marked point; if not, we try again and repeat the process.

Our main goal is to understand the scaling of the cost/complexity of the algorithm. To do so, we must state precisely what task is to be completed, the algorithm to achieve the task, which parts of the algorithm do and do not contribute to its cost, and how much the former cost. We will see that some of these costs are ignored in the discrete search algorithms. Thus:

**Task.** *Present a point  $x \in M$ , a homogeneous Riemannian manifold of finite volume, that with probability  $1 - \delta$  satisfies  $w \in N(x, \epsilon)$  – that is,  $w$  is contained in a neighborhood of size  $\epsilon$  of  $x$ .*

What type of neighborhood  $N(x, \epsilon)$  one uses will have to be specified for each particular manifold  $M$ , and need not be the standard metric balls  $B(x, \epsilon)$  coming from some metric  $d$  on  $M$ . We consider  $1/\text{vol}(N(x, \epsilon))$  to be the “size of the problem” (since  $\text{vol}(M)/\text{vol}(N(x, \epsilon))$  is the number of  $\epsilon$ -neighborhoods you could fit into  $M$ ). Thus, we let the “size of the database” grow by locating  $w$  to greater and greater precision.

When one speaks of the  $\sqrt{N}$  complexity of Grover’s algorithm, one is referring to the query complexity of the algorithm: how many queries to the oracle one must make in order to find the marked item. In the analog search algorithms, the potential marking the marked point is the “oracle,” and the “complexity” is given by how long it takes to find the marked point – sometimes called the “query time.” This is known as the Hamiltonian oracle model [Moc07]. We will likewise consider the query complexity of our algorithm to be the total amount of time we must keep the potential turned on. In the discrete case, because checking whether the item  $x_i$  is the marked item  $w$  is not considered to contribute to the cost of the algorithm, how long it takes to find the marked point and how long the potential is turned on coincide. In our case, however, the potential is on during the check phase as well as the search phase, and thus the cost is not simply given by how

long we let the particle evolve on  $M$ .

Having specified what we will consider contributing to the cost of performing the algorithm, we make two notes. First, there are a number of tuneable parameters in our algorithm. The cost will depend on the values to which those parameters have been tuned. In particular, for each  $\epsilon$ , there will be an optimal set of parameter values. Second, we will consider the complexity to be the expected cost. Again, this is similar to how analog search is analyzed: when success probabilities cannot reach 1, the algorithm is run several times until the marked point is found. So we will be looking for the parameters that optimize the expected cost of the algorithm. Working out the final formula for the expected cost will be done over the course of the rest of the chapter, as the various details of our algorithm are filled in.

We now give an overview of the search phase.

## 2.1 Search Phase

As we described, many search algorithms can be broken into two alternating phases: a search phase and a check phase. During the search phase, a candidate point  $x$  is somehow produced, and one checks to see if  $x$  is the marked point  $w$ . If it is, you're done. If it isn't, you repeat: run the search phase again to come up with another candidate  $x'$ , which you then proceed to check.

In the original Grover search algorithm, the search is done by a particle hopping from lattice site to lattice site according to the graph Laplacian, a dis-

cretization of the Schrödinger equation. In the analog algorithms, the Schrödinger equation is also used, this time giving the differential equations that describe the continuous evolution of the probability amplitudes of each lattice site. We mimic those searches by letting a particle evolve on  $M$  according to the Schrödinger equation for some amount of time, and then performing a position measurement to find a candidate point  $x$ .

**Definition 2.1.1.** The search phase on  $M$  is given by a particle prepared in the uniform state  $\psi(x) = 1/\sqrt{\text{vol}(M)}$  evolving according to the Hamiltonian

$$H\psi = -\gamma_s\Delta\psi - \delta_w\psi,$$

which describes the Schrödinger equation on  $M$ .

Note that we've specified the form our potential takes: it's merely a Dirac delta potential located at  $w$ . We had said that the potential should depend on  $w$  so that it could be used to locate  $w$ . A potential supported solely on  $w$  intuitively seems to be the most sensible way of doing that. Although we could use other potentials – a constant potential on some small neighborhood of  $w$ , or a Gaussian sharply concentrated around  $w$ , for instance – we find there are two advantages to a delta potential. First, some of the analysis during the check phase would be greatly complicated by any other potential; we shall see later why that is. Second, during the check phase, we will be restricting ourselves to  $\epsilon$ -neighborhoods, which will become increasingly smaller, and we will require our potential to be supported on a subset of those neighborhoods. With a delta potential, we sidestep the issues

regarding how to weigh the cost of a changing potential. Admittedly, there is a potential downside to using a delta function: above dimension one, delta potentials must be constructed using the theory of self-adjoint extensions. Also, it is well-known that for some spaces, a delta potential is “invisible” (*e.g.*, the Laplacian on  $\mathbb{R}^n$  minus the origin is essentially self-adjoint for  $n \geq 4$ , meaning there is no difference between the case of a delta potential at the origin and no potential at all); this may be true for other manifolds in certain dimensions.

We have now mentioned or alluded to two of the tuneable parameters in the algorithm:

**Definition 2.1.2.** Let  $t_s \in \mathbb{R}_{\geq 0}$  be the tuneable parameter describing how long the particle searches before its position is measured.

**Definition 2.1.3.** Let  $\gamma_s = \frac{1}{2m} \in \mathbb{R}_{>0}$  be the tuneable parameter describing the inverse mass of the particle of the search phase.

Note that there is no parameter specifying the strength of the potential. This is because, as in the other search algorithms, the coefficient on the potential can be absorbed into  $\gamma_s$ . (This is discussed further in Section 4.2.)

Before turning to the check phase, we will discuss the cost of our algorithm and work out the cost of the search phase. As we mentioned, we will work out the formula for the cost bit by bit over the next several pages.

We recall that we are interested in the scaling of the *average query time* of our algorithm. Since the algorithm alternates between search phases and check

phases until a check confirms we've found  $w$ , the time it will take to find  $w$  is random, depending on how many tries it takes for the particle to be measured near it. Thus, to find the expected cost, we condition on the number of tries it takes. By the Law of Total Expectation, we have

$$\mathbb{E}(\text{cost}) = \sum_{k \geq 1} \mathbb{E}(\text{cost} \mid k \text{ tries})P(k \text{ tries}). \quad (2.1)$$

We introduce a new parameter (though not a tuneable one!):

**Definition 2.1.4.** The probability of the particle being within  $\epsilon$  of  $w$  is given by

$$p_\epsilon = \int_{N(w, \epsilon)} |\psi(x, t_s)|^2 dx.$$

The number of tries required to find  $w$  during the search phase is a geometric random variable with parameter  $p_\epsilon$ ; we may hence write

$$\mathbb{E}(\text{cost}) = \sum_{k \geq 1} \mathbb{E}(\text{cost} \mid k \text{ tries})(1 - p_\epsilon)^{k-1}p_\epsilon. \quad (2.2)$$

The cost of the search phase of the algorithm is simple to calculate. The potential is left on for time  $t_s$  while the particle evolves according to the Schrödinger equation; hence, if it takes  $k$  tries to find  $w$ , the search phase contributes  $kt_s$  to the cost. Splitting the cost into the contributions from the two phases as  $\text{cost}_s + \text{cost}_c$ , the expected cost (2.2) becomes

$$\mathbb{E}(\text{cost}) = \sum_{k \geq 1} \left( kt_s + \mathbb{E}(\text{cost}_c \mid k \text{ tries}) \right) (1 - p_\epsilon)^{k-1} p_\epsilon. \quad (2.3)$$

This is not the final formula for the cost; we will continue to work it out. Furthermore, even once we have worked it out as much as possible, for a specific manifold and  $\epsilon$ , the cost will still depend on the choices of the various parameters.

We now turn to the check phase.

## 2.2 Check Phase

After the search phase, we need a way to check if the measured location  $x$  of the searching particle is within  $\epsilon$  of the marked point  $w$ . At first glance, this seems to not be particularly difficult. If we suppose we could impose an infinite potential outside of  $N(x, \epsilon)$ , we could place a particle inside of  $N(x, \epsilon)$  and restrict our attention solely to the neighborhood. What we would then have is a “particle in a box” on the manifold  $M$  – either with or without a delta potential, depending on if  $x$  has been located close enough to  $w$ . The energy levels of the system would differ based on whether or not a delta potential existed within  $N(x, \epsilon)$ . Thus, to check whether or not a delta potential is within  $N(x, \epsilon)$ , we could make an energy measurement of the system and see which of the two spectra the result belongs to.

Though this may seem to address the situation, it is actually not sufficient for our purposes. In the axiomatic formulation of quantum mechanics, making a measurement is an operation one is assumed to be able to perform. Making measurements in a real life experiment is different. In the real world, in order to make an energy measurement, we shine a laser tuned to a particular frequency at the system and see whether it fluoresces. To compute the cost of the check phase of the algorithm, we must know how long it takes to perform the energy measurement as a function of the neighborhood’s size,  $\epsilon$ . To do so, we model a laser shining on a

charged particle as a particle in a box with a perturbation given by an oscillating EM field. We approximate this system as a two-level quantum system, consisting of the ground state and the first excited state (in the case of a degeneracy leading to multiple “first” excited states, we can orient the field to break the symmetry, resolving the degeneracy). The field can drive oscillations of the system between the two levels; the effectiveness depends on its frequency being tuned close to the excitation energy of the system. This phenomenon is known as Rabi oscillation.

We tune the frequency of the field to the excitation energy of the particle in a box when there’s no delta potential inside it. If we prepare the system in its ground state and turn on the field, the field will drive oscillations between the two states of the system. To “measure the fluorescence,” we measure the system after letting it evolve for some amount of time  $t_c$  (say, by flipping on a photodetector and seeing if a photon is released from the system due to stimulated emission). We find the system either in the ground state or the excited state. Since the frequency was tuned to that of the system when there is no potential, the probability of finding the system in the excited state is usually greater in the case that there’s no potential (this is not actually always true, and we must be careful to select parameters so that it is). In general, it is possible to find the system in either state, regardless of whether or not the potential is present; however, the probabilities for the two cases differ. Thus, we can perform the procedure many times to get a distribution of measurement results, and then perform statistical analysis on the distribution in order to determine if there’s a potential in the system or not.



It follows that the cost of each check of whether we've found the potential will simply be  $nt_c$ , where  $n$  is the number of the Rabi oscillation measurements needed to perform the statistical analysis. If it takes  $k$  instances of searching and checking to find the potential, then the total cost associated with checking will be  $knt_c$  (we assume the cost of a check is the same when the potential is there as when it isn't, since the potential will be turned on in either case). This means

$$\begin{aligned}
\mathbb{E}(\text{cost}) &= \sum_{k \geq 1} \left( kt_s + \mathbb{E}(\text{cost}_c \mid k \text{ tries}) \right) (1 - p_\epsilon)^{k-1} p_\epsilon \\
&= \sum_{k \geq 1} k(t_s + nt_c) (1 - p_\epsilon)^{k-1} p_\epsilon \\
&= (t_s + nt_c) / p_\epsilon.
\end{aligned} \tag{2.4}$$

We note that we haven't associated a cost to the preparation of the particle in a box system on  $N(x, \epsilon)$ . As the both the particle's energy and the energy gap between the ground and excited state increase with smaller  $\epsilon$ , it should get only easier to prepare the system in its ground state. Therefore, whatever cost does exist does not contribute to the scaling of the overall cost.

We now work out some of the details.

A particle of charge  $q$  evolving according to the Schrödinger equation in  $N(x, \epsilon)$  with a driving field and potential has the Hamiltonian

$$H\psi = -\gamma_c \nabla \psi - V(x)\psi - (q\vec{E}(t) \cdot \vec{x})\psi.$$

In our case, either  $V(y) = \delta_w(y)$  if  $w \in N(x, \epsilon)$ , or  $V(y) = 0$ . Let  $|g\rangle, |e\rangle$  be the ground and first excited states of the system (either  $|g_n\rangle, |e_n\rangle$  if there's no

potential, or  $|g_p\rangle, |e_p\rangle$  if there is); let the driving field  $\vec{E}(t)$  have amplitude and frequency given by  $A \cos \omega t$ . Now let us approximate the system as a two-level quantum system.

**Definition 2.2.1.** Let  $t_c \in \mathbb{R}_{\geq 0}$  be the tuneable parameter describing how long the particle evolves before a measurement is made to see if the system is found in state  $|g\rangle$  or state  $|e\rangle$ .

**Definition 2.2.2.** Let  $\gamma_c = \frac{1}{2m} \in \mathbb{R}_{>0}$  be the tuneable parameter describing the inverse mass of the charged particle of the check phase.

The unperturbed Hamiltonian will be given by

$$H_0 = \begin{pmatrix} E_g & 0 \\ 0 & E_e \end{pmatrix},$$

which is equivalent to

$$H = \begin{pmatrix} 0 & 0 \\ 0 & E_e - E_g \end{pmatrix} = \begin{pmatrix} 0 & 0 \\ 0 & \Delta E \end{pmatrix},$$

as they differ by a multiple of the identity. (Again, we note that the energies and the energy gap depend on whether or not a potential is present:  $\Delta E$  is either  $\Delta E_p$  or  $\Delta E_n$ .) The driving (time-dependent) Hamiltonian is of the form

$$H_{int}(t) = \begin{pmatrix} 0 & dqA \cos \omega t \\ d^*qA \cos \omega t & 0 \end{pmatrix},$$

where  $d = \langle g|X|e\rangle$ . From here on, we'll absorb the  $q$  into the  $A$ .

Note that the value of  $d$  will depend on  $N(x, \epsilon)$  (and also whether or not there's a potential). This is the usual set up for Rabi oscillations. It follows from a standard calculation that if the system is prepared in the state  $|g\rangle$  and evolves according to the Hamiltonian  $H = H_0 + H_{int}$ , the probability of finding the system in the state  $|e\rangle$  upon measurement after time  $t_c$  is given by

$$p_e(t_c) = \frac{(dA)^2}{\Omega_R^2} \sin^2\left(\frac{\Omega_R}{2}t_c\right), \quad (2.5)$$

where  $\Omega_R = \sqrt{(dA)^2 + \Delta^2}$  is the Rabi frequency and  $\Delta = \omega - \Delta E$  is the detuning [Ste07]. Recall that we choose  $\omega$  to equal  $\Delta E_n$ , the energy gap in the case where there's no potential, and that  $d$ ,  $\Delta$ ,  $\Delta E$  (and hence  $\Omega_R$ ) all depend on whether or not there's a potential.

There are a few things to note about (2.5). First, if the detuning  $\Delta$  is 0, the sine-squared curve has amplitude 1. Conversely, as the detuning gets larger, the Rabi frequency increases, while the amplitude goes to 0. Lastly, it is also important to note that making  $A$  larger increases the Rabi frequency without decreasing the amplitude. However,  $A$  isn't allowed to be a tuneable parameter, as we were only allowed a single tuneable parameter in discrete quantum search. Therefore, we fix some value of  $A$ ; arbitrarily increasing  $A$  wouldn't be physically reasonable.

In order to determine whether or not  $w \in N(x, \epsilon)$ , we let the Rabi system evolve for time  $t_c$  and then measure. The system will be measured in the state  $|e\rangle$  with probability

$$p_1 = p_1(t_c) = \sin^2\left(\frac{\Omega_{R,n}}{2}t_c\right) = \sin^2\left(\frac{d_n A}{2}t_c\right)$$

if the detuning is 0, *i.e.*, if the potential is not there, or with probability

$$p_2 = p_2(t_c) = \frac{(d_p A)^2}{\Omega_{R,p}^2} \sin^2\left(\frac{\Omega_{R,p}}{2} t_c\right)$$

if it is; otherwise, we observe  $|g\rangle$ .

We find ourselves sampling from a random variable which can take on the two values – in other words, a Bernoulli random variable, with  $|g\rangle$  and  $|e\rangle$  corresponding to 0 and 1, respectively. The problem, however, is we don't know whether we're sampling from  $X_1 \sim B(p_1)$  or  $X_2 \sim B(p_2)$ . We can collect some number  $n$  of samples before we attempt to determine which case we're in. Let  $X \sim B(n, p)$  be the binomial variable given by the  $n$  trials. If after  $n$  measurements, we've observed  $|e\rangle$   $k$  times, the maximum likelihood estimate for  $p$  is given by  $\hat{p} = \frac{k}{n}$ . Assuming  $n$  is sufficiently large (relative to how much  $p_1, p_2$  differ), the estimate for  $p$  should be closer to whichever of  $p_1$  and  $p_2$   $p$  actually is. If we know  $p_1$  and  $p_2$ , then our decision rule should lead us to conclude we're sampling from  $X_i$  if  $\hat{p}$  is closer to  $p_i$ . Thus, if  $\hat{p} < (p_1 + p_2)/2$ , we assume  $p = p_2$ , meaning there is a delta potential inside  $N(x, \epsilon)$ , meaning we've found  $w$ ; otherwise, we haven't located  $w$ , and the search must go on.

Unfortunately, we come upon a complication: the decision rule we just came up with depends on knowing  $p_2$  (so that we may know the average of  $p_1$  and  $p_2$ ). But  $p_2$  depends on the detuning  $\Delta$ , which in turn depends on the energy gap of the system, which itself in turn depends on where the delta potential is located inside of  $N(x, \epsilon)$ . As the potential gets closer to the boundary of  $N(x, \epsilon)$ , the

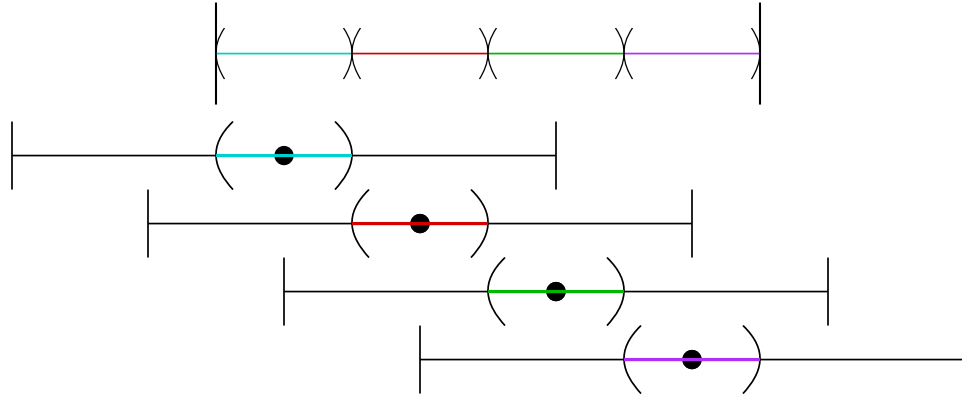


Figure 2.1: If we do  $R = 4$  checks with overlapping intervals, no point in the original interval will be further than  $r = \epsilon/8$  from the center of one of the overlapping intervals

detuning will tend to 0, meaning  $p_2$  will tend towards  $p_1$ , and hence making it difficult to distinguish between “potential” case and the “no potential” case when the potential is located near the boundary.

Our solution is to, in essence, force the potential to be sufficiently far from the boundary of the neighborhood, allowing us to have a lower bound on the detuning. Obviously, we can neither pick where  $w$  nor  $N(x, \epsilon)$  is; however, we chose to create the system of a particle in the box with a field at  $N(x, \epsilon)$ , and we’re free to create such a system wherever we choose. Namely, we can create many such systems in such a way that the small neighborhoods of their center cover  $N(x, \epsilon)$ . By choosing these neighborhoods so that they are sufficiently overlapping, we can guarantee that if  $w$  is in  $N(x, \epsilon)$ , then it will be inside of one of these new systems and at least a given distance from its boundary.

More specifically, there’s a function relating  $r = d(w, x)$  to the detuning  $\Delta$ . If we want to guarantee that  $\Delta$  will be at least some minimal value, that specifies a

value of  $r$ . Then we can cover  $N(x, \epsilon)$  with new overlapping neighborhoods  $N(x_i, \epsilon)$  so that no point of  $N(x, \epsilon)$  is further than  $r$  away from one of the  $x_i$  (that is, the  $x_i$  form an  $r$ -net). There's some  $R$  that's the minimal size of an  $r$ -net; since we'll have to make  $R$  checks for this single run of the check phase, the cost associated with the check phase will be multiplied by  $R$ :

$$\mathbb{E}(\text{cost}) = (t_s + nt_c)/p_\epsilon = (t_s + nRt_c)/p_\epsilon.$$

(Note the slight abuse of notation: in the first expression  $n$  is the total number of times the Rabi oscillation measurements were necessary for the statistical analysis in the check phase, but now is the number of times they are necessary to perform the analysis for each of the  $R$  sub-checks.)

As a result of this, we have a guarantee that in at least one of the overlapping neighborhoods, the detuning is above some bound, and hence  $p_2$  is below some bound. In the statistical analysis, we may act as if that bound always holds for  $p_2$ , because if some of the overlapping neighborhoods contain the potential but the actual  $p_2$  is larger than the bound, we merely mistakenly think there's no potential. As a result, we continue looking for it in the subsequent overlapping neighborhoods, until we come to the one for which  $p_2$  is actually below the bound we're using, and we correctly recognize we've located the potential.

## Statistical Analysis

We now work out the details involved in determining whether we are sampling from the “no-potential” distribution  $X_1 \sim B(p_1)$  or the “potential” distribution  $X_2 \sim B(p_2)$ . To perform one of the  $R$  checks, we collect  $n$  samples and look at  $\hat{p}$ , the fraction of measurements finding the particle in the excited state  $|e\rangle$ . We need to figure out how large  $n$  needs to be.

As there’s only a  $p_\epsilon$  chance that the search phase has output a point near  $w$ , it’s likelier that when we are performing our analysis we are in the case that there is no potential. In the language of hypothesis testing, we will let the “no potential” case be our null hypothesis:

- $H_0$ : there is no potential in the neighborhood  $N$ , so we’re sampling from  $X_1 \sim B(p_1)$ , and the random variable  $X \sim B(n, p)$  of all the Rabi measurements is a binomial with  $p = p_1$ .
- $H_a$ : there is a potential in the neighborhood  $N$ , so we’re sampling from  $X_2 \sim B(p_2)$ , and the random variable  $X \sim B(n, p)$  of all the Rabi measurements is a binomial with  $p = p_2$ .

Let  $\alpha$  and  $\beta$  denote the Type I and Type II error rates: the probability of mistakenly rejecting  $H_0$  and of mistakenly failing to reject  $H_0$ , respectively. Recall that we are assuming that it’s on the  $k$ th try that we finally locate  $w$ . That has implications for when and how often we are allowed to make Type I and Type II errors.

Now we need to work out what  $n$ ,  $\alpha$ , and  $\beta$  need to be in order to ensure a success probability greater than  $1 - \delta$ . Suppose it takes  $k$  tries to find  $w$ . There are many ways that could happen: every time before the  $k$ th try, we can either find  $w$  but fail to realize it, or not find  $w$  and correctly recognize that's the case. If we only take into account instances where we make no mistakes at all, we get our first relation:

**Proposition 2.2.3.** *If the Type I and Type II error rates  $\alpha, \beta$  satisfy*

$$\frac{p_\epsilon(1 - \beta)}{1 - (1 - p_\epsilon)(1 - \alpha)} = 1 - \delta, \quad (2.6)$$

*then the success probability is at least  $1 - \delta$ .*

*Proof.* Succeeding while making no mistakes is a subevent of succeeding generally. Therefore we sum the probabilities of finding  $w$  on the  $k$ th try without making any mistakes:

$$\begin{aligned} P(\text{success}) &> P(\text{no mistakes}) = \sum_{k \geq 1} \left( (1 - p_\epsilon)(1 - \alpha) \right)^{k-1} p_\epsilon(1 - \beta) \\ &= \frac{p_\epsilon(1 - \beta)}{1 - (1 - p_\epsilon)(1 - \alpha)} = 1 - \delta, \end{aligned} \quad (2.7)$$

□

The second relation comes from setting the Type I and Type II error rates equal to  $\alpha$  and  $\beta$ .

**Proposition 2.2.4.** *Suppose one is trying to tell if  $Y \sim B(p_1)$  or  $Y \sim B(p_2)$  by collecting  $n$  samples from  $Y$  and using the decision rule of selecting whichever of*



$p_1, p_2$  the max-likelihood estimate  $\hat{p}$  is closer to. Then if  $n$  satisfies

$$n = \max \left( -\frac{2 \ln(\alpha)}{\Delta p^2}, -\frac{2 \ln(\beta)}{\Delta p^2} \right), \quad (2.8)$$

the Type I and Type II error rates will be bounded by  $\alpha$  and  $\beta$ , respectively.

*Proof.* Recall  $p$  is the parameter of the Bernoulli we're sampling from in the Rabi measurements; it's also the parameter of  $X$ , the binomial variable consisting of all the samples. We have

$$\begin{aligned} \alpha &= P(\text{mistakenly think there's a potential}) \\ &= P(\hat{p} < (p_1 + p_2)/2 \mid p = p_1) \\ &= P(X < n(p_1 + p_2)/2 \mid X \sim B(n, p_1)) \\ &= P(X - np_1 < -\frac{n\Delta p}{2}) \\ &\leq e^{-n\Delta p^2/2} \end{aligned}$$

where  $\Delta p = p_1 - p_2$ , and the last line follows from the Hoeffding inequality. Similarly,

$$\begin{aligned} \beta &= P(\text{fail to realize there's a potential}) \\ &= P(\hat{p} > (p_1 + p_2)/2 \mid p = p_2) \\ &= P(X - np_2 > \frac{n\Delta p}{2}) \\ &\leq e^{-n\Delta p^2/2}. \end{aligned}$$

Rearranging and solving for  $n$ , the result follows.  $\square$

**Corollary 2.2.5.** *Given the assumptions above,  $n$  will be minimized if  $\alpha = \beta$  and*

$$\alpha = \beta = 1 - \frac{1 - \delta}{p_\epsilon + (1 - p_\epsilon)(1 - \delta)},$$

*giving us*

$$n = -\frac{2 \ln(\alpha)}{\Delta p^2}.$$

*Proof.* Looking at (2.6), we see that if  $\delta$  and  $p_\epsilon$  are held fixed, setting a value for one of  $\alpha$  or  $\beta$  determines what the other must be for the relation to be satisfied, and that increasing one will decrease the other. That means that the minimal  $n$  satisfying (2.8) will occur when the two arguments are equal, which occurs when  $\alpha$  and  $\beta$  are equal. Combining that fact with (2.6), the result follows.  $\square$

# Chapter 3

## Quantum Search on $S^1$

In this chapter we analyze quantum search on the circle.

### 3.1 Search Phase

We wish to solve the Schrödinger equation with a delta potential on  $S^1$ .

What follows is standard.

The Schrödinger equation on the circle is equivalent to the Schrödinger equation on an interval with periodic boundary conditions. Let  $I = [-\frac{a}{2}, \frac{a}{2}]$  and  $S^1(a) = I/\partial I$ . The Hamiltonian of the system is given by

$$H\psi(x) = -\gamma_s\psi''(x) - \delta_w(x),$$

where  $w \in I$  is the marked point we are searching for. We may assume  $w = \frac{a}{2}$  as we proceed to solve the equation – moving the potential from  $w$  to  $w'$  will merely rotate the solutions by  $w' - w$ .

To solve the equation, we look for solutions to the eigenvalue problem  $H\psi = E\psi$  that are continuously differentiable, except possibly at  $w$ . Since the potential is located only at  $x = \frac{a}{2}$ , we have

$$-\gamma_s \psi''(x) = E\psi(x)$$

for  $x \neq \frac{a}{2}$ . The solutions are of the form  $Ae^{ikx} + Be^{-ikx}$  for  $k$  satisfying  $E = \gamma_s k^2$  and for  $x \in I - \frac{a}{2}$ ; by continuity, it holds at  $x = \frac{a}{2}$ , as well. These solutions must satisfy a number of conditions. The periodic boundary conditions mean we have

$$A(e^{ik\frac{a}{2}} - e^{-ik\frac{a}{2}}) - B(e^{ik\frac{a}{2}} - e^{-ik\frac{a}{2}}) = 0. \quad (3.1)$$

Integrating both sides of  $-\gamma_s(Ae^{ikx} + Be^{-ikx})'' = E\psi(x)$  across an  $\epsilon$ -neighborhood of the potential and letting  $\epsilon \rightarrow 0$ , we get

$$A(e^{ik\frac{a}{2}} - e^{-ik\frac{a}{2}} - \frac{1}{ik\gamma_s}e^{ik\frac{a}{2}}) + B(e^{ik\frac{a}{2}} - e^{-ik\frac{a}{2}} - \frac{1}{ik\gamma_s}e^{ik\frac{a}{2}}) = 0. \quad (3.2)$$

(Note the right hand side vanishes due to the (assumed) continuity of  $\psi(x)$ .) Examining (3.1), we see that either  $A = B$ , or  $e^{ik\frac{a}{2}} - e^{-ik\frac{a}{2}} = 0$  and  $ka$  is an integer multiple of  $2\pi$ , *i.e.*,  $k = \frac{2\pi n}{a}$ . If the former holds, then (3.2) implies (after some simplification)

$$-2k\gamma_s = \cot\left(\frac{ka}{2}\right) \quad (3.3)$$

if  $E$  is positive, and

$$2p\gamma_s = \coth\left(\frac{pa}{2}\right) \quad (3.4)$$

if  $E$  is negative and  $k = ip$  is imaginary.

If, on the other hand, we have  $k = \frac{2\pi n}{a}$ , we see that (3.2) reduces to

$$A\left(-\frac{1}{ik\gamma_s}e^{ik\frac{a}{2}}\right) + B\left(-\frac{1}{ik\gamma_s}e^{ik\frac{a}{2}}\right) = 0,$$

and we thus have  $A = -B$ . We will see shortly that we may ignore this case.

As the hyperbolic tangent is an odd function that monotonically decreases from  $\infty$  to 1 on the positive reals, we see that (3.2) has two opposite solutions; thus there is a single eigenfunction  $\psi_0(x) = A_0e^{px} + A_0e^{-px} = 2A_0 \cosh(px)$ , the sole bound state of the system. There are infinitely many eigenfunctions coming from (3.1), as a line will intersect the cotangent function infinitely many times; again, the solutions come in opposite pairs, so that there is one eigenfunction  $\psi_j(x) = A_j e^{ik_j x} + A_j e^{-ik_j x} = 2A_j \cos(k_j x)$  for each period of  $\cot(\frac{ka}{2})$ . If we let

$$A_j = \sqrt{\frac{ak_j + \sin ak_j}{2k_j}}$$

and

$$A_0 = \sqrt{\frac{ap + \sin ap}{2p}},$$

the eigenfunctions  $A_j \cos(k_j x)$  will properly normalized. This characterizes all the eigenfunctions of the Hamiltonian.

Finding all the eigenfunctions means we've solved the system: if the system is prepared in the initial state

$$\psi(x, t = 0) = \sum_0^\infty \langle \psi_j | \psi \rangle \psi_j(x),$$

the linearity of time evolution means that at time  $t$  the system will be in the state

$$\psi(x, t) = \sum_0^\infty \langle \psi_j | \psi \rangle \psi_j(x) e^{-iE_j t}.$$

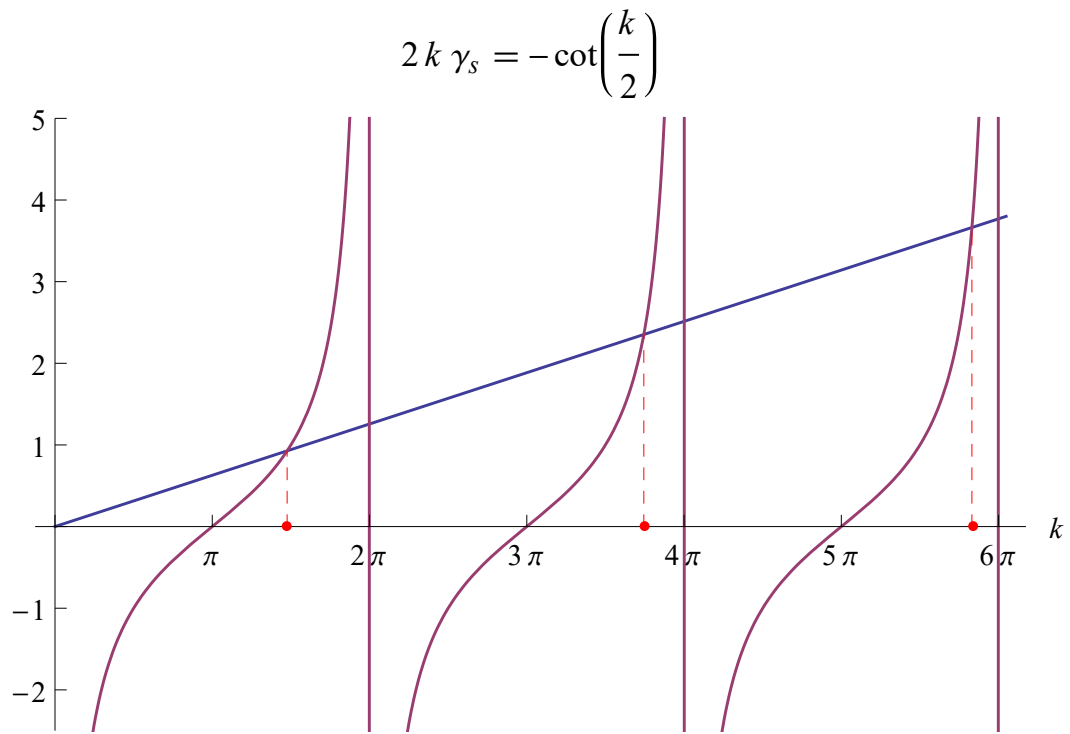


Figure 3.1: Quantization condition for unbound states

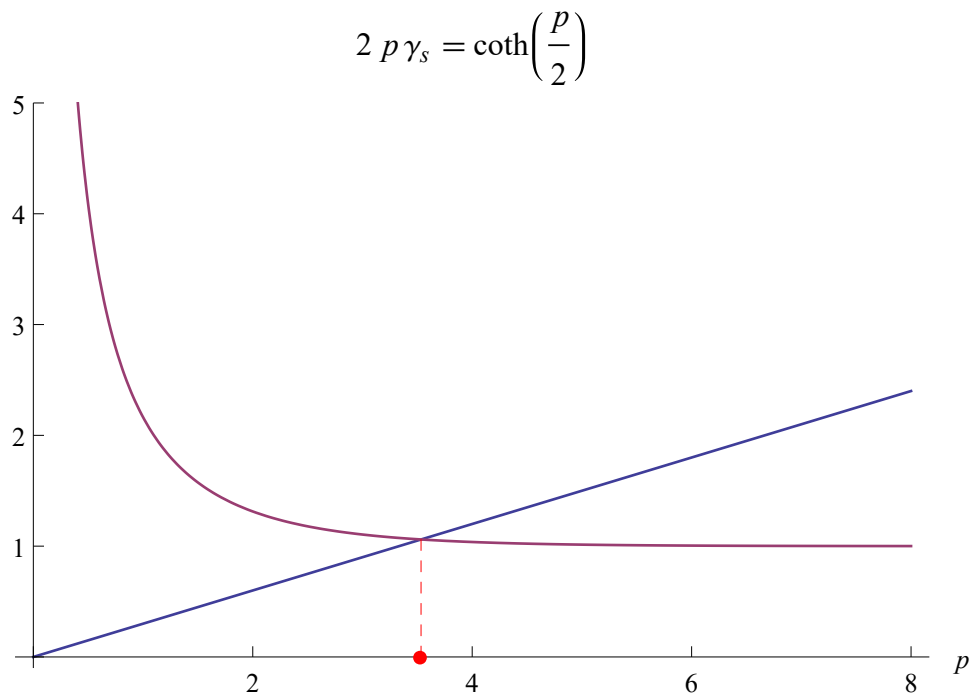


Figure 3.2: Quantization condition for the bound state

Now we are able to see why we were able to ignore the case where  $A = -B$ : we wish to initialize the system with the uniform distribution  $s(x) = \frac{1}{\sqrt{a}}$ , an even function which has no projection onto the odd sine and sinh eigenfunctions that would have followed.

To find  $p_\epsilon(t)$ , we integrate the square modulus of  $\psi(x, t)$ . Writing  $\psi(x, t) = \sum_0^\infty c_j \psi_j(x) e^{-iE_j t}$ , we have

$$|\psi(x, t)|^2 = \sum c_j \psi_j(x) e^{-iE_j t} \overline{\sum c_l \psi_l(x) e^{-iE_l t}} = \sum c_j \bar{c}_l \psi_j(x) \bar{\psi}_l(x) e^{-i(E_j - E_l)t},$$

and thus

$$p_\epsilon(t) = \sum c_j \bar{c}_l e^{-i(E_j - E_l)t} \int_{\frac{a}{2} - \epsilon}^{\frac{a}{2} + \epsilon} \psi_j(x) \bar{\psi}_l(x) dx.$$

## 3.2 Check Phase

For the check phase, we need to solve two systems: a particle in a box, and a particle in a box with a potential located at an arbitrary location. We wish to understand the difference between the energy gaps of the two systems, as this controls the detuning, which affects the distinguishability of the two systems.

The former is well-known to have solutions which are sinusoidal functions completing an integer multiple of half periods. More precisely, the eigenfunctions of the Schrödinger equation on the interval  $[0, L]$  are of the form  $\psi_n(x) = A \sin(k_n x) = A \sin(\frac{n\pi}{L} x)$ , where  $A$  is the normalizing constant. If the interval were shifted, then the solutions would be shifted by the same amount.

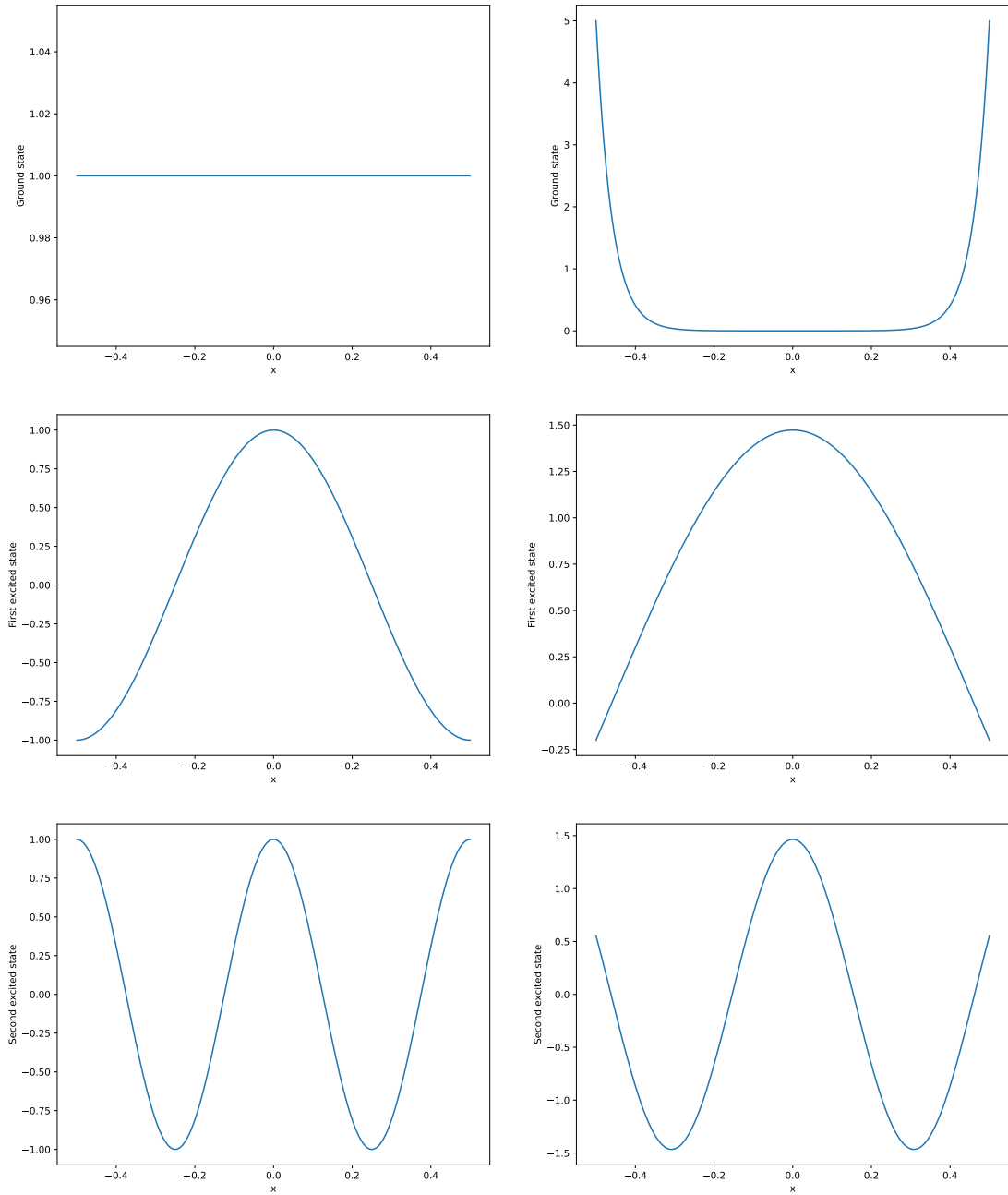


Figure 3.3: Comparing the first three eigenstates for a particle on a circle with (second column) and without (first column) a delta potential. The the second and third plots of first column actually show a linear combination of eigenstates for the energies  $E_1$  and  $E_2$ , which are degenerate with multiplicity 2.



The ground state and the first excited state are  $A \sin(\frac{\pi}{L}x)$  and  $A \sin(\frac{2\pi}{L}x)$ .

The energy levels are given by  $E_j = \gamma_c k_j^2 = \gamma_c \frac{j^2 \pi^2}{L^2}$ , and so the energy gap is  $\Delta E_n = 3\gamma_c \frac{\pi^2}{L^2}$ . Thus, the unperturbed Hamiltonian is

$$H_0 = \begin{pmatrix} 0 & 0 \\ 0 & E_e - E_g \end{pmatrix} = \begin{pmatrix} 0 & 0 \\ 0 & \Delta E_n \end{pmatrix} = \begin{pmatrix} 0 & 0 \\ 0 & 3\gamma_c \frac{\pi^2}{L^2} \end{pmatrix}.$$

The driving term of the Hamiltonian has a  $d_n = \langle g_n | X | e_n \rangle$  in it, which can easily be calculated to be  $\frac{16L}{9\pi^2}$ . Therefore, we have

$$H_{int}(t) = \begin{pmatrix} 0 & \frac{16L}{9\pi^2} A \cos \omega t \\ \frac{16L}{9\pi^2} A \cos \omega t & 0 \end{pmatrix}.$$

We can now write  $p_1(t)$ , the probability of finding the particle to be in state  $|e\rangle$  during a Rabi check. Recall, we have

$$p_1 = p_1(t_c) = \sin^2\left(\frac{\Omega_{R,n}}{2} t_c\right) = \sin^2\left(\frac{d_n A}{2} t_c\right),$$

so  $p_1(t_c) = \sin^2\left(\frac{16A}{18\pi^2} L t_c\right)$ . The  $L$  in the numerator means that as  $\epsilon$  shrinks, keeping  $p_1$  constant requires waiting proportionally longer until the first time  $p_1(t)$  hits that value.

This was all for the particle in a box system, when there's no potential. We move on to the next case, when the potential is present.

Now we wish to find (continuously differentiable, except possibly at  $w$ ) solutions to the Schrödinger equation on  $[0, L]$  with a delta potential at an arbitrary point  $w \in [0, L]$ . The solutions for this system are also known, though perhaps not so commonly. In fact, the procedure to find them is similar to the calculation in the

previous section, when we solved the Schrödinger equation with a delta potential on the circle. Briefly: We know that the solutions vanish at the endpoints and are sine waves away from  $w$ . We have two sine waves: one on  $[0, w]$ , one on  $[w, L]$ . By continuity, they must agree at  $w$ , but there can be a discontinuity in the derivative.

Integrating

$$-\gamma_c \psi'' - \delta_w \psi = E \psi$$

across a tiny neighborhood of  $w$  and letting it shrink gives the discontinuity in the derivative. Enforcing the discontinuity in the derivative leads to the quantization condition on the wavenumbers of the solutions.

The solutions are given by

$$\psi(x) = \begin{cases} A \sin(kx) & x \in [0, w] \\ B \sin(k(x - L)) & x \in [w, L] \end{cases}$$

for  $A, B$  satisfying  $A \sin(kw) = B \sin(k(w - L))$  and  $k$  satisfying

$$\gamma_c k = \frac{\sin(kw) \sin(kL - kw)}{\sin(kL)}. \quad (3.5)$$

There can be a negative energy solution (a bound state), corresponding to imaginary  $k$ . If  $k = ip$ , the quantization condition becomes

$$\gamma_c p = \frac{\sinh(pw) \sinh(pL - pw)}{\sinh(pL)}, \quad (3.6)$$

and the solution is as above, but with hyperbolic sines. Plotting the negative energy quantization condition, we see that there is a bound state only if the slope of the line,  $\gamma_c$ , is small enough to make the line intersect the RHS; taking the

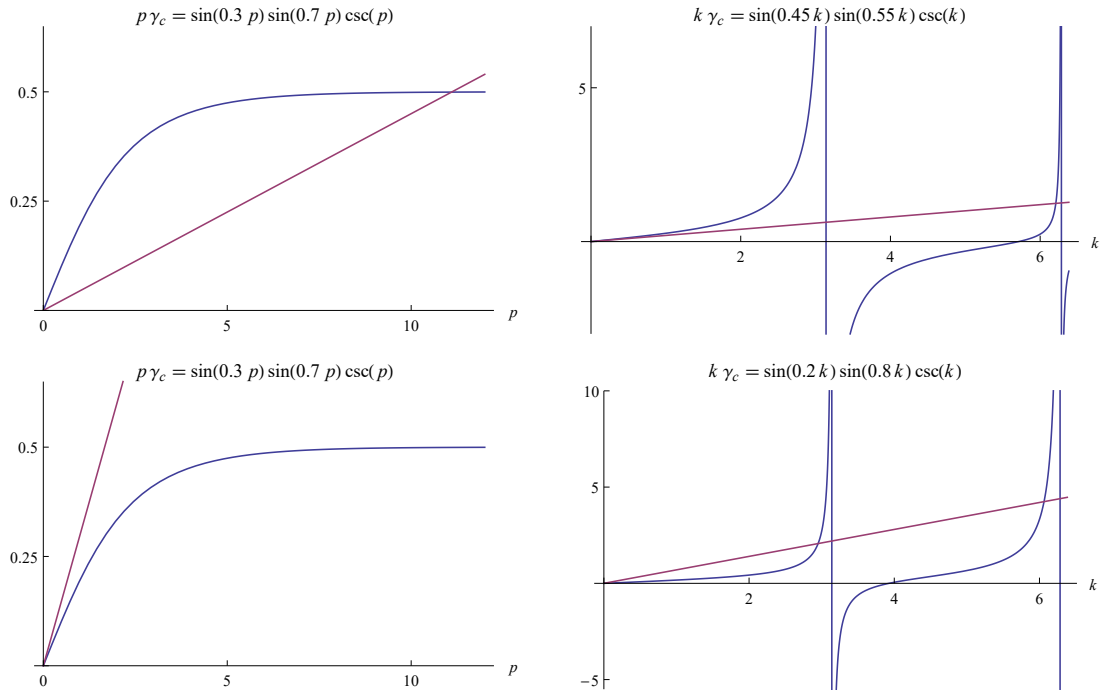


Figure 3.4: Quantization condition for the unbound and bound states for different values of  $\gamma_c$ ; the first row satisfies  $\gamma_c < w(L - w)/L$ , while the second does not.

derivative of the RHS at 0 shows the condition is  $\gamma_c < w(L - w)/L$ . Doing the same with the quantization condition in the regular case, we see that  $\gamma_c$  being small enough for there to be a bound state means that that line will miss intersecting the RHS of the quantization condition during the first “period” (before the first asymptote). Thus, the ground state is either the bound state or the solution with wavenumber from the first “period”, and the first excited state is the solution with wavenumber from the second period.

Computing  $\Delta E_p$ ,  $d_p$ , and hence the detuning  $\Delta$  and  $p_2(t)$  will result in nasty formulas due to the dependence of the system on the location of the potential,  $w$ , and whether or not the ground state  $|g_p\rangle$  is a bound state. There are a few facts about them, however, which will be relevant in establishing analytic results in

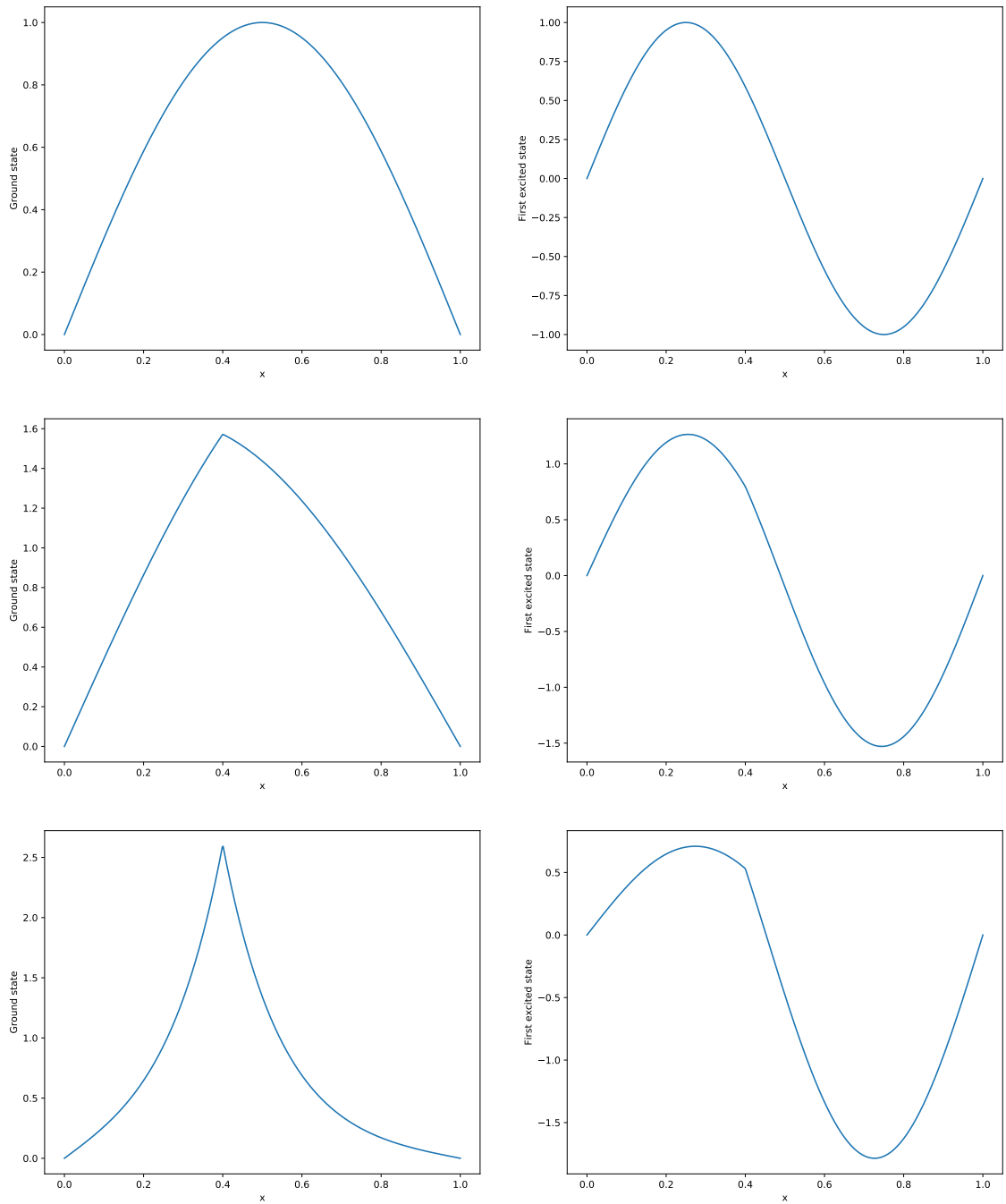


Figure 3.5: The first two eigenstates for a particle in a box without (first row) and with a delta potential (second and third rows). The second and third rows have different values of  $\gamma_c$ ; the third row satisfies the condition so that the ground state is a bound state.

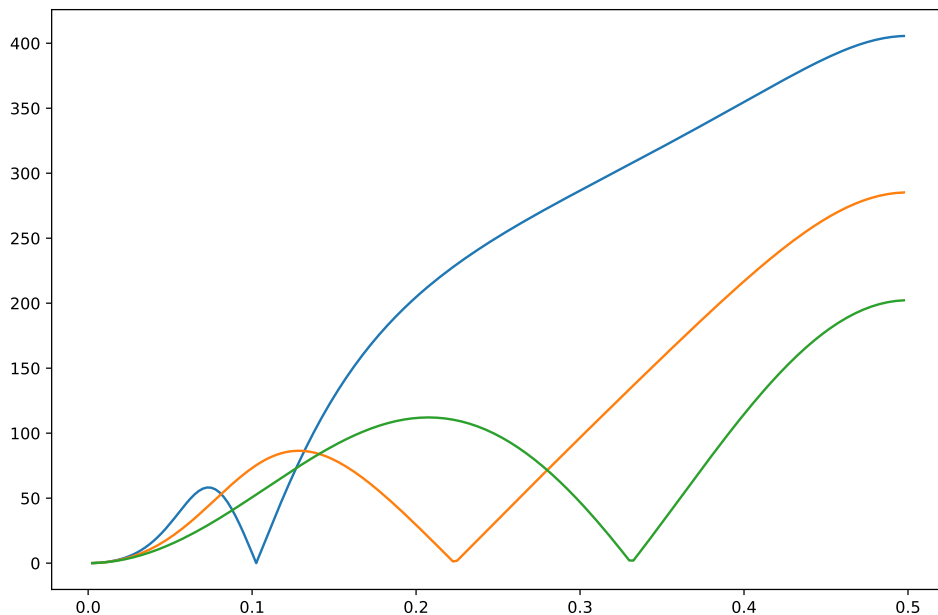


Figure 3.6: A plot of the detuning  $\Delta$  as a function of what proportion of the way into the box  $w$  is, for three different values of  $\gamma_c$ . Note that  $\Delta$  grows as  $w$  approaches the center of the box, and this effect is stronger for smaller  $\gamma_c$ .

the next section – some may be easily seen numerically, while others follow from tedious calculations that are easily done with the aid of symbolic computation software.

First, we can see numerically that the detuning  $\Delta$  is largest in magnitude when  $w = L/2$ . This informs our efforts to do overlapping checks to ensure that the potential is within  $r$  of the center of the interval during one of the checks. Furthermore, the mere fact that  $\Delta$  is non-zero means that, by continuity, it will be bounded away from zero for sufficiently small  $r$ .

Second, using symbolic computation software, we can see that  $d_p$  will also have a factor of  $L$  in it, in the case that  $|g_p\rangle$  isn't a bound state (which requires that  $\gamma_c$  must be sufficiently large to avoid a solution to the negative energy quantization

condition). What is important about this is that  $d_p$  will shrink as  $\epsilon$  does. (In fact, we can establish this fact using the theory of self-adjoint extensions, which we use in the next chapter. For now, we'll simply assert that  $d_p$  has a factor of  $L$  in it.)

### 3.3 Analytic Results

We show that with particular choices of the various parameters, it's possible work out how the expected cost of the algorithm will scale as  $\epsilon$  goes to 0. This isn't necessarily the optimal choice of parameters, and hence this result is about the Big O scaling of the cost, not the Big Theta scaling – that is, this merely an upper bound on the scaling.

We work out the scaling over the course of a few simple results. First we get a simple formula for  $p_\epsilon$ .

**Proposition 3.3.1.** *There is a choice of parameters so that  $p_\epsilon$  scales as  $c\epsilon + o(\epsilon)$  as  $\epsilon$  goes to 0.*

*Proof.* If we let  $t_s = 0$ , the initial probability distribution is uniform on the space, and  $p_\epsilon$  is simply  $2\epsilon / \text{vol}(M)$ . □

Using that result, we can find the scaling of  $\alpha$ , the Type I and Type II error rates of the statistical analysis during the check phase. Recall we consider the cost a function of  $N = 1/\epsilon$ .

**Proposition 3.3.2.** *If  $p_\epsilon$  scales as above, then  $-\ln(\alpha)$ , the numerator of  $n =$*

$-\frac{2\ln(\alpha)}{\Delta p^2}$  (the number of checks necessary in order to achieve error rate  $\alpha$ ), will scale as  $\ln(c\frac{1}{\epsilon}) = \ln(cN)$ .

*Proof.* We have

$$\begin{aligned}\alpha &= 1 - \frac{1 - \delta}{p_\epsilon + (1 - p_\epsilon)(1 - \delta)} \\ &= \frac{p_\epsilon \delta}{p_\epsilon \delta + (1 - \delta)} \\ &= \frac{1}{1 + (1 - \delta)/p_\epsilon \delta} = \frac{1}{1 + \frac{\delta'}{p_\epsilon}},\end{aligned}$$

where  $\delta' = (1 - \delta)/\delta$ . Then  $\ln(\alpha) = \ln(\frac{1}{1 + \delta'/p_\epsilon}) = -\ln(1 + \delta'/p_\epsilon)$ . If  $p_\epsilon$  scales as  $c\epsilon + o(\epsilon)$ , then  $-\ln(\alpha)$  scales as

$$\ln\left(\frac{\delta'}{c\epsilon + g(\epsilon)}\right) = \ln(\delta') - \ln(c\epsilon + g(\epsilon)),$$

where  $g(\epsilon)$  is  $o(\epsilon)$ . That means

$$\begin{aligned}\ln(\delta') - \ln(c\epsilon + g(\epsilon)) &= \ln(\delta') - \ln(\epsilon(c + \tilde{g}(\epsilon))) \\ &= \ln(\delta') - \ln(\epsilon) - \ln(c + \tilde{g}(\epsilon)) \\ &= \ln\left(\frac{\delta'}{\epsilon}\right) + \ln\left(\frac{1}{c + \tilde{g}(\epsilon)}\right),\end{aligned}$$

where the second term is bounded above by  $\ln(1/c)$ , since  $\tilde{g}(\epsilon)$  tends to 0. Therefore,  $-\ln(\alpha)$  will scale as  $\ln\left(\frac{\delta'}{\epsilon}\right) = \ln(\delta'N)$ .  $\square$

Now we deal with  $\Delta p^2$ .

**Proposition 3.3.3.** *There is a choice of parameters so that  $\Delta p$  (which is in the denominator of  $n = -\frac{2\ln(\alpha)}{\Delta p^2}$ ) is bounded away from 0 as  $\epsilon$  goes to 0.*

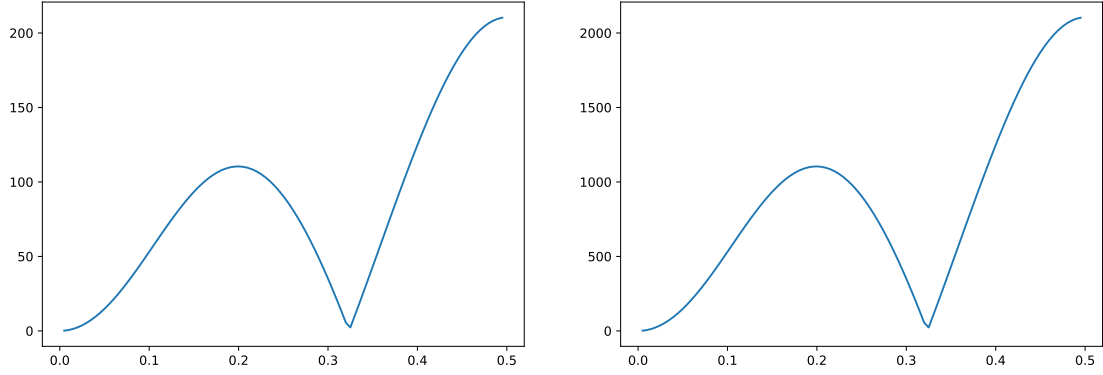


Figure 3.7: Scaling  $\gamma_c$  and  $\epsilon$  by the same factor (in this case, 10) will scale the detuning  $\Delta$  by that factor.

*Proof.* To bound  $\Delta p^2$  from below, we can fix  $p_1$  and then show that  $p_2$  can be bounded away from it.

Fixing  $p_1$  is easy:  $p_1(t_c) = \sin^2(\frac{16A}{18\pi^2}Lt_c)$  depends only on  $L$  and  $t_c$ . If we grow  $t_c$  to keep  $Lt_c$  fixed (*i.e.*, keep  $\epsilon t_c$  fixed), then  $p_1$  will remain fixed. Note that this means that  $t_c$  will scale as  $1/\epsilon = N$ .

To bound  $p_2$ , first we recall from (2.5) that

$$p_2(t) = \frac{(d_p A)^2}{\Omega_{R,p}^2} \sin^2\left(\frac{\Omega_{R,p} t}{2}\right) = \frac{(d_p A)^2}{\Delta^2 + (d_p A)^2} \sin^2\left(\frac{\Omega_{R,p} t}{2}\right),$$

which is clearly bounded by  $\frac{(d_p A)^2}{\Delta^2 + (d_p A)^2}$ . We know from the previous section that  $d_p$  shrinks as  $\epsilon$  does. Thus, if we can show that  $\Delta$  is growing, we'll have  $p_2$  shrinking as  $\epsilon$  goes to 0.

The detuning  $\Delta$  is  $\Delta E_p - \Delta E_n$ , since we set the frequency of the field,  $\omega$ , equal to  $\Delta E_n$ . Recall we have  $\Delta E_n = 3\gamma_c \frac{\pi^2}{L^2}$ , and  $\Delta E_p = \gamma_c(k_2^2 - k_1^2)$ , for  $k_1, k_2$  the wavenumbers of  $|g_p\rangle, |e_p\rangle$ . We have to analyze how these scale with  $\epsilon$ .



First, note that the wavenumbers are solutions to

$$\gamma_c k = \frac{\sin(kw) \sin(kL - kw)}{\sin(kL)}$$

(or the same equation with hyperbolic sines, in the bound state case). If we let  $p = w/L$  denote the location of the potential as a fraction of the length of the interval, we can replace  $w$  with  $pL$  in the equation to get

$$\gamma_c k = \frac{\sin(kpL) \sin(kL - kpL)}{\sin(kL)}.$$

Now if we let  $\gamma_c$  scale like  $\epsilon$ , we see that the wavenumbers solving the quantization condition will scale like  $1/\epsilon$ . Since  $\Delta E_p = \gamma_c(k_2^2 - k_1^2)$  has two powers of  $L$  in the denominator from the  $k_i$ , but one power of  $L$  in the numerator due to  $\gamma_c$ , it will scale like  $1/\epsilon$  for each fixed  $w$  or  $p$ . If we scale  $r$  so that we know for one of the checks we have the potential within a fixed proportion of the length of the interval of the center,  $R$  will remain fixed, and whatever lower bound we have for  $\Delta$  will scale like  $1/\epsilon$ . Thus,  $\Delta$  will be growing and  $d_p$  will be shrinking as  $\epsilon$  goes to 0, meaning  $p_2$  will go to 0, and  $\Delta p^2$  will go to  $p_1^2$ .  $\square$

We are finally in place to derive the scaling of the cost of the algorithm.

**Proposition 3.3.4.** *There is a choice of parameters so that  $\mathbb{E}(\text{cost}) = (t_s + nRt_c)/p_\epsilon$  is  $O(N^2 \ln N)$ .*

*Proof.* If we combine the last three propositions, we get

$$\begin{aligned}
\mathbb{E}(\text{cost}) &= (t_s + nRt_c)/p_\epsilon \\
&= (t_s - \frac{2 \ln(\alpha)}{\Delta p^2} R \frac{t'_c}{\epsilon})/c\epsilon \\
&= \frac{1}{c} N (t_s + \frac{2 \ln(\delta' N)}{\Delta p^2} R t'_c N),
\end{aligned} \tag{3.7}$$

whose highest order term is  $\frac{2Rt'_c}{c\Delta p^2} N^2 \ln(\delta' N)$ . □

### 3.4 Numerical Results

We have numerical results that suggest that the scaling of the previous section is indeed optimal. We ran a simulated annealing algorithm to estimate the optimal values of the parameters for a range of values of  $\epsilon$ . The cost appears to scale like  $O(N^2 \ln N)$ .

To estimate  $p_\epsilon$ , we took the first 400 solutions to the quantization condition to approximate the evolution of the uniform state, and numerically integrated it over an  $\epsilon$ -neighborhood of  $w$ . Approximations to the quantization condition were necessary in order to solve it while avoiding overflows/underflows due to the hyperbolic trig functions, which grow or shrink exponentially. For large  $\gamma_s$ , the solution to the quantization condition for the bound state moves closer to 0, and thus we can replace the  $\coth \frac{x}{2}$  with its two term series expansion about 0,  $\frac{2}{x} + \frac{x}{6}$ . Similarly, for large  $\gamma_s$ , the solutions to the quantization condition move closer to the asymptotes of  $\cot \frac{x}{2}$ , meaning the cotangent looks like a shifted  $\frac{2}{x}$ . Both of these cases are easily solved by hand for  $k$ . In the case of small  $\gamma_s$ , the solution

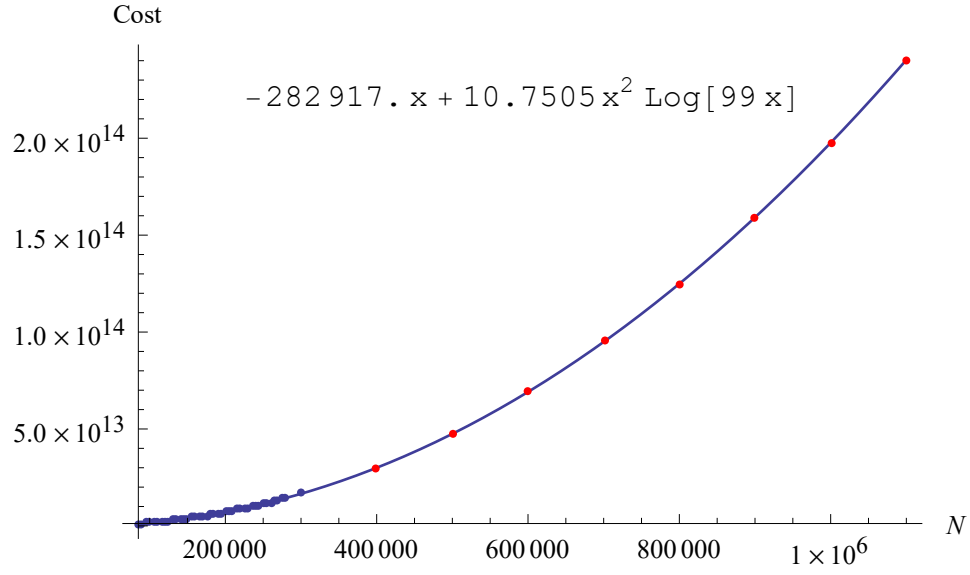


Figure 3.8: A list plot of the cost and the best fit of the form  $aN^2 \log \delta' N + bN$ . The function was fit on the blue data; it matches the rest of the data (in red) quite well.

to the bound state quantization condition becomes large. Since  $\coth \frac{x}{2}$  shrinks exponentially to 1, we just set it equal to 1 and solve  $2\gamma_s k = 1$  for  $k$ . Lastly, if the bound state  $\cosh kx$  has wave number  $k$  that is large, we use an approximation in constructing the wave function. The first term in the expansion of the wave function as a series,  $\langle \psi_0 | 1 \rangle \psi_0$ , is approximated by  $2 \exp k(x - \frac{1}{2})$ , to avoid the overflow from having hyperbolic sines in the denominator.

As we saw in the last section, the detuning  $\Delta$  grows and  $d_p$  shrinks as  $\epsilon$  shrinks. Because of this, we know that  $p_2$  shrinks to 0 as  $\epsilon$  does, and so we neglected  $p_2$  and set  $\Delta p$  equal to  $p_1$ . As a result, there is no reason to pick a smaller value for  $r$  and hope for a possibly better runtime – the potential gains were due to the large detuning giving a smaller bound on  $p_2$ , and thus making  $\Delta p$  larger. Hence, we picked  $r$  to be the largest value for which the detuning is strictly positive for

all smaller values of  $r$ .

The simulated annealing started at a temperature of 1 and cooled by a factor of .9 after every 100 steps, until reaching a temperature of 0.000001. The steps in  $t_s$ ,  $\gamma_s$ , and  $\gamma_c$  were exponential: the jump in the exponent was a uniformly random variable over a range that scaled down with the temperature. The jumps in  $t_c$  were a uniformly random variable over a range that scaled up as  $\epsilon$  shrank and scaled down with the temperature.

During the simulated annealing optimization, we kept track of the best value of the parameters during the process, not just taking the values at the end. We ran the simulated annealing algorithm multiple times (at least five) for each value of  $\epsilon$  and kept the best result.

Though the cost seems to be well-fit by a  $N^2 \log N$  curve, that alone doesn't show that the points are actually being generated by such a curve. Other evidence, however, strongly suggests that that is actually the case and that the analytic result of the last section is in fact optimal. What we find is that the naïve choice of parameters we made in the last section is in fact the same as what the simulated annealing algorithm found. In particular,  $\gamma_s$  doesn't scale with  $\epsilon$ ; the values cluster around 2. Similarly,  $t_s$  doesn't scale, either; it clusters around 0.7. This matches our choice of keeping  $\gamma_s$  and  $t_s$  fixed, so that  $p_\epsilon$  would scale like  $\epsilon$ . Furthermore,  $t_c$  grows linearly, exactly as we chose in order to keep  $p_1$  fixed. Lastly, though  $\gamma_c$  varies wildly, all the values correspond to a detuning that leads to  $r = .495$ .

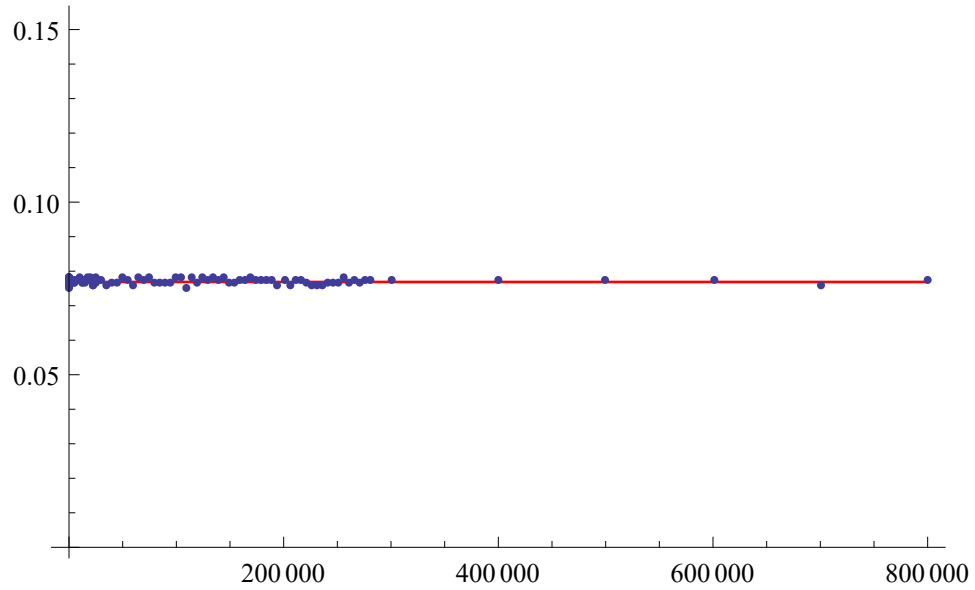


Figure 3.9: A list plot of  $\gamma_s$ , along with its mean.  $\gamma_s$  and  $t_s$  are held nearly constant, mimicking the strategy used for the analytic scaling.

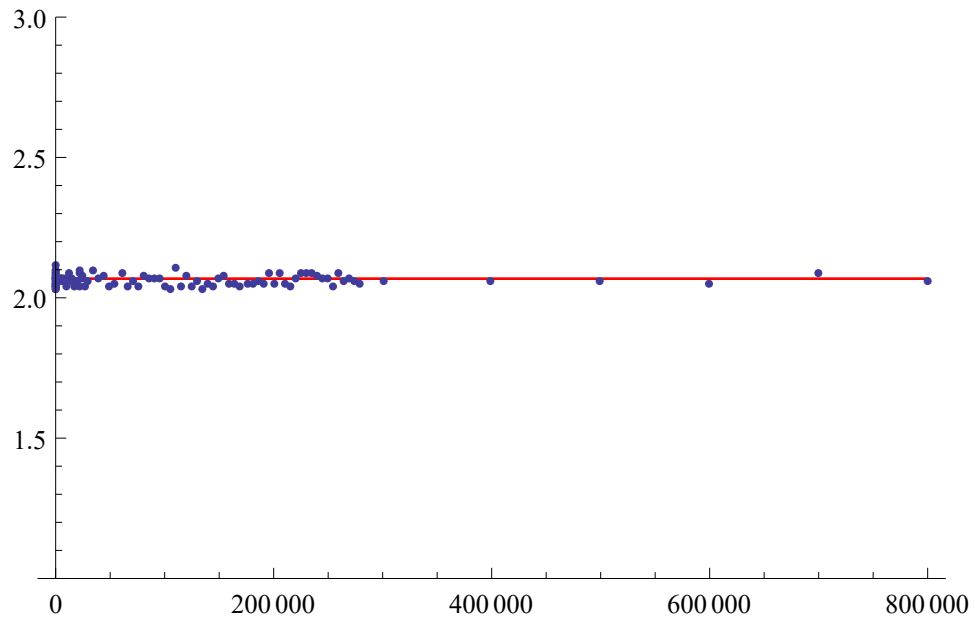


Figure 3.10: A list plot of  $t_s$ , along with its mean.  $t_s$  and  $\gamma_s$  are held nearly constant, mimicking the strategy used for the analytic scaling.

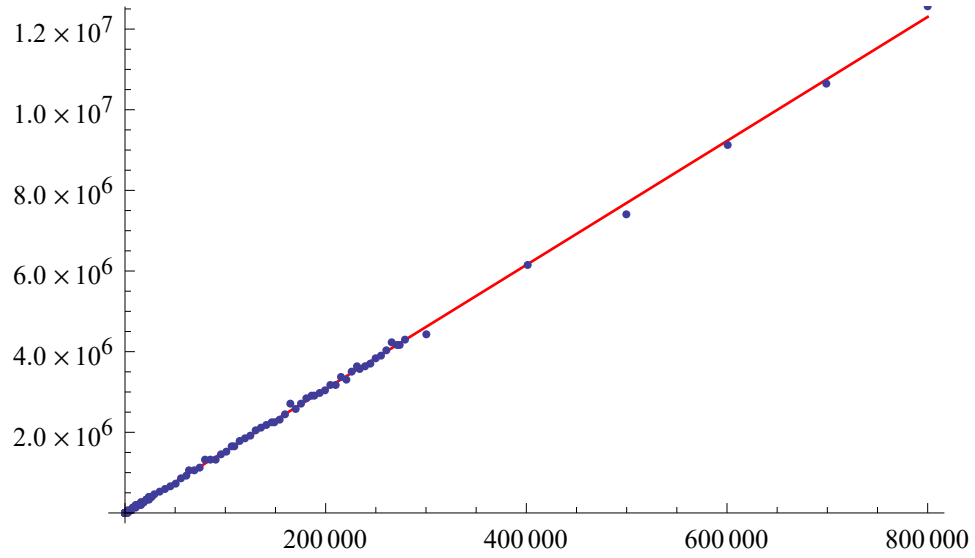


Figure 3.11: A list plot of  $t_c$ , along with the line of best fit.  $t_c$  grows nearly linearly, mimicking the strategy used for the analytic scaling.

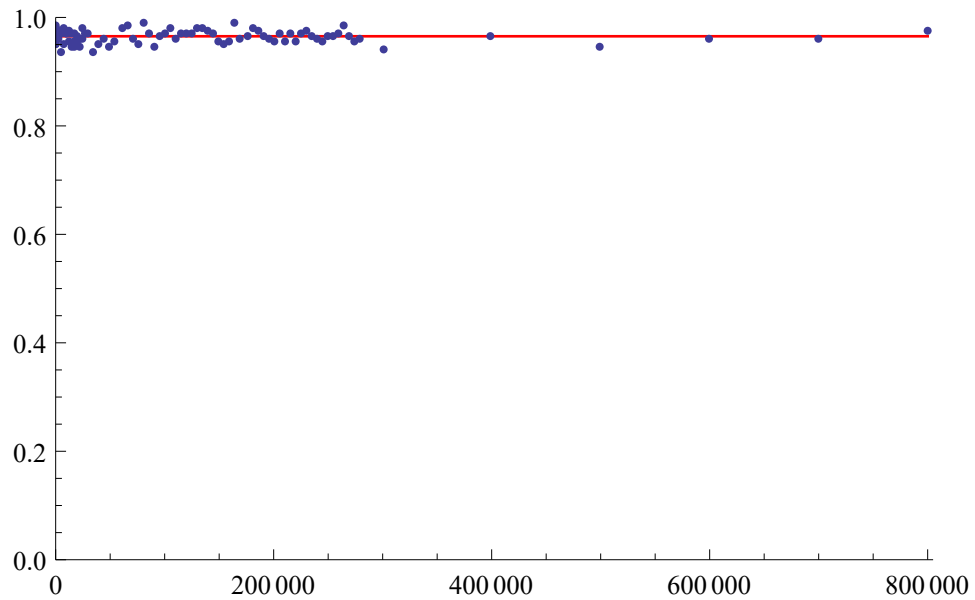


Figure 3.12: A list plot of  $p_1$ , along with its mean. It is nearly constant as a result of  $t_c$  growing nearly linearly, mimicking the strategy used for the analytic scaling.

# Chapter 4

## Quantum Search on $T^2$

In this chapter we analyze quantum search on the torus.

### 4.1 Self-adjoint Extensions

In moving up a dimension, we find ourselves faced with difficulties in defining the Hamiltonian that corresponds to the Schrödinger equation with a delta potential. A self-adjoint operator with the heuristic form  $-\Delta + \lambda\delta$  must be found using the von Neumann's theory of deficiency indices and self-adjoint extensions. It will turn out that there's an entire family of self-adjoint operators corresponding to a perturbation of the Laplacian by a point interaction or delta potential; the family is indexed by a parameter  $\eta$  which corresponds to the renormalized strength or coupling constant of the potential.

We give a very brief overview of the theory; for a thorough discussion, see

the textbooks by Reed and Simon [RS75] or Hall [Hal13].

**Definition 4.1.1.** Let  $A$  be a densely-defined operator  $A : \mathcal{H} \rightarrow \mathcal{H}$ . If the functional  $\langle v, A- \rangle$  is bounded, then  $v$  is in  $\text{Dom}(A^*)$ , and  $A^*v$  is the unique vector  $z$  such that  $\langle v, A- \rangle = \langle z, - \rangle$ .  $A^*$  is called the adjoint of  $A$ .

**Definition 4.1.2.** A densely-defined operator  $A : \mathcal{H} \rightarrow \mathcal{H}$  is symmetric if for all  $v, w \in \text{Dom}(A)$ ,  $\langle v, Aw \rangle = \langle Av, w \rangle$ .

Symmetric operators are not the same as self-adjoint operators.

**Definition 4.1.3.** A densely-defined operator  $A$  is self-adjoint if it is symmetric and  $\text{Dom}(A) = \text{Dom}(A^*)$ .

Though the difference may seem minor at first glance, it is a crucial one: the spectral theorem holds for self-adjoint operators, but not operators that are merely symmetric.

**Definition 4.1.4.** Let  $A$  be a densely-defined symmetric operator. The deficiency subspaces of  $A$  are  $K_{\pm} = \ker(A^* \mp i)$ , and the deficiency indices of  $A$  are  $n_{\pm} = \dim(K_{\pm})$ .

We present the core facts regarding self-adjoint extensions in the following theorem.

**Theorem 4.1.5.** *A closed densely-defined symmetric operator  $A$  is self-adjoint if and only if  $n_{\pm} = 0$ .  $A$  has self-adjoint extensions if and only if  $n_+ = n_-$ ; there*



is an infinite family of self-adjoint extensions in one-to-one correspondence with the unitary maps from  $K_+$  to  $K_-$ . Given such a unitary  $U$ , the domain of the corresponding extension  $A_U$  is

$$\{\varphi + \varphi_+ + U\varphi_+ \mid \varphi \in \text{Dom}(A), \varphi_+ \in K_+\}.$$

The extension  $A_U$  acts on its domain by

$$\varphi + \varphi_+ + U\varphi_+ \mapsto A\varphi + i\varphi_+ - iU\varphi_+.$$

If  $A$  has  $n_{\pm} = 0$  but isn't closed, we say it is essentially self-adjoint, and just replace it with its closure, which is self-adjoint by the theorem above.

## 4.2 Delta Potentials in 2D

We now present the results applying the theory of self-adjoint extensions to the Schrödinger equation with a delta potential. The two cases we need – a rectangle in  $\mathbb{R}^2$  and the flat torus – are handled at the same time; enforcing periodic boundary conditions for the rectangle will handle the torus. The problems of self-adjoint extensions on a rectangle or torus were studied by Šeba [Šeb90], whose work relied on earlier results by Zorbas [Zor80]. Our exposition largely follows that of Lee [Lee16].

Consider the two systems given by the Hamiltonian  $H = -\Delta$  on the Hilbert space of  $L^2$  functions on  $[0, L] \times [0, L]$  that are either zero on the boundary, or have periodic boundary conditions. Let  $\varphi_n(\vec{x}), \lambda_n$  denote the (normalized) eigenpairs of

$H$ . In order to create a delta potential at  $\vec{w}$ , we restrict the domain of  $H$  to those functions vanishing at  $\vec{w}$  (which do not sense the presence of the potential at  $\vec{w}$ ). Label the restriction of  $H$  as  $H_0$ ; this is the symmetric operator whose self-adjoint extensions will correspond to the Laplacian with a delta potential.

Applying the self-adjoint extension theory to  $H_0$ , we get a 1-parameter family of self-adjoint extensions  $H_{\eta, \vec{w}} = -\Delta_{\eta, \vec{w}}$ , for  $\eta \in (-\infty, \infty]$ . We will drop the  $\vec{w}$  and just refer to the extension as  $H_\eta = -\Delta_\eta$ . The parameter  $\eta$  can be thought of as a renormalized inverse potential strength; namely,  $\eta = \infty$  corresponds to the Laplacian without a potential.

It should be noted that in the previous two chapters, the strength of the potential was held fixed at  $-1$ , and the tuneable parameter  $\gamma$  was the coefficient on the Laplacian. In this case, however, we will let  $\eta$  be the tuneable parameter, rather than  $\gamma$ , for reasons that will be made clear in Section 4.5. Tuning  $\eta$  rather than  $\gamma$  still leaves us with one parameter determining the Hamiltonian. Furthermore, there is a sense in which the two choices of tuneable parameter are equivalent: in the end, it's their ratio that matters. The Schrödinger equation with a potential is of the form  $\partial_t \psi = aA\psi + bB\psi$ . Dividing through by  $a$  or  $b$  gives  $\frac{1}{a}\partial_t \psi = A\psi + \frac{b}{a}B\psi$  or  $\frac{1}{b}\partial_t \psi = \frac{a}{b}A\psi + B\psi$ ; we can absorb the coefficient on the  $\partial_t$  into  $t$  and change the time variable to  $t'$  and let  $\frac{a}{b}$  or  $\frac{b}{a}$  be the sole tuneable parameter of our Hamiltonian.

We now address the spectrum and eigenspaces of  $H_\eta$ . Eigenvalues  $z \in \sigma(-\Delta_\eta)$  come in two types: those also in  $\sigma(-\Delta)$  (unperturbed eigenvalues), and new ones (perturbed eigenvalues).

Unperturbed eigenvalues appear because eigenfunctions vanishing at  $\vec{w}$  do not feel the presence of a delta potential located at  $\vec{w}$  (*i.e.*, they're unperturbed by the delta potential), and thus should still be eigenfunctions of the extension. Thus,  $z \in \sigma(-\Delta_\eta) \cap \sigma(-\Delta)$  if and only if the multiplicity of  $z$  as an eigenvalue of  $-\Delta$  is greater than 1 or  $-\Delta$  has an eigenfunction corresponding to  $z$  that vanishes at  $\vec{w}$ . The eigenspace of  $z \in \sigma(-\Delta_\eta) \cap \sigma(-\Delta)$  is given by

$$\left\{ \sum c_n \varphi_n \mid \sum c_n \varphi_n(\vec{w}) = 0, -\Delta \varphi_n = z \varphi_n \right\};$$

its dimension is one less than the multiplicity of  $z \in \sigma(-\Delta)$ .

Perturbed eigenvalues appear with multiplicity 1 and satisfy a quantization condition for  $-\Delta_\eta$ ,  $F(z) = \eta$ , where

$$F(z) = \sum_{n=1}^{\infty} |\varphi_n(\vec{w})|^2 \left( \frac{1}{\lambda_n - z} - \frac{\lambda_n}{\lambda_n^2 + 1} \right),$$

and, as mentioned before,  $\varphi_n, \lambda_n$  are the eigenpairs of  $-\Delta$ . The (unnormalized) eigenfunction corresponding to  $z$  has  $L^2$  expansion

$$\psi_z = \sum_{n=1}^{\infty} \frac{\overline{\varphi_n(\vec{w})}}{\lambda_n - z} \varphi_n.$$

It turns out that the eigenvalues of  $-\Delta_\eta$  interlace those of  $-\Delta$ : we have  $z_1 \leq \lambda_1 \leq z_2 \leq \lambda_2 \leq \dots$ . It is also true that the unperturbed eigenvalues have multiplicity one less than they do in  $\sigma(-\Delta)$ . The equality in the interlacing is due to unperturbed eigenvalues – the perturbed eigenvalues fall strictly between the eigenvalues of  $-\Delta$  (assuming  $\eta$  is finite).

We note a few similarities between the quantization conditions for the circle/interval and the torus/rectangle. Both have solutions that are given by finding the intersections of a line with a function that is monotonic on intervals bounded by asymptotes. Since the first eigenvalue  $z_1 \in \sigma(-\Delta_\eta)$  is between  $-\infty$  and  $\lambda_1 > 0$ , depending on the value of  $\eta$ , it's possible for  $z_1$  to be negative for the rectangle. Thus, the ground state of the system may or may not be a bound state with negative energy. For the torus, however, the ground state is the constant function, which has energy 0.

### 4.3 Search Phase

The search phase is given by a particle on  $T^2 = \mathbb{R}^2/L\mathbb{Z}^2$  (which we think of as  $[0, L] \times [0, L]$  with the *Asteroids* boundary conditions) evolving according to the Hamiltonian given formally by  $H = -\Delta + c\delta_{\vec{w}}$ . We may assume  $\vec{w} = (0, 0)$ , since we can just translate the results. We begin with  $H = -\Delta$  on the Hilbert space of  $L^2$  functions on  $[0, L] \times [0, L]$  with periodic boundary conditions, and obtain the self-adjoint extensions  $H_\eta = -\Delta_\eta$ .

The eigenvalues and eigenfunctions of  $-\Delta_\eta$  are given in terms of those of  $-\Delta$ . It's well known that for any  $\vec{n} \in \mathbb{Z}^2$ ,  $\varphi_{\vec{n}}(\vec{x}) = \frac{1}{L^2} \exp\left(\frac{2\pi i}{L} \vec{n} \cdot \vec{x}\right)$  is an eigenfunction with eigenvalue  $\frac{4\pi^2}{L^2} (n_1^2 + n_2^2)$  and that together they form an orthonormal basis. Most (all but one, in fact) of the eigenvalues have multiplicity greater than 1, due to the symmetries  $(n_1, n_2) \mapsto (\pm n_1, \pm n_2)$ ,  $(n_1, n_2) \mapsto (\pm n_2, \pm n_1)$ . These appear

as unperturbed eigenvalues of  $-\Delta_\eta$  with eigenspace given by linear combinations vanishing at  $\vec{0}$  of unperturbed eigenfunctions.

There are also the perturbed eigenvalues  $z$  solving the quantization condition

$$\begin{aligned}\eta &= \sum_{\vec{n} \in \mathbb{Z}^2} |\varphi_{\vec{n}}(\vec{0})|^2 \left( \frac{1}{\lambda_{\vec{n}} - z} - \frac{\lambda_{\vec{n}}}{\lambda_{\vec{n}}^2 + 1} \right) \\ &= \sum_{\vec{n} \in \mathbb{Z}^2} |\varphi_{\vec{n}}(\vec{0})|^2 \left( \frac{1}{4\pi^2 \|\vec{n}\|^2 / L^2 - z} - \frac{4\pi^2 \|\vec{n}\|^2 / L^2}{16\pi^4 \|\vec{n}\|^4 / L^4 + 1} \right) \\ &= \sum_{\vec{n} \in \mathbb{Z}^2} |\varphi_{\vec{n}}(\vec{0})|^2 \left( \frac{L^2}{4\pi^2 \|\vec{n}\|^2 - L^2 z} - \frac{4\pi^2 \|\vec{n}\|^2 L^2}{16\pi^4 \|\vec{n}\|^4 + L^4} \right).\end{aligned}$$

The corresponding unnormalized eigenfunction is

$$\begin{aligned}\psi_z &= \sum_{\vec{n} \in \mathbb{Z}^2} \frac{\overline{\varphi_{\vec{n}}(\vec{0})}}{\lambda_{\vec{n}} - z} \varphi_{\vec{n}} \\ &= \sum_{\vec{n} \in \mathbb{Z}^2} \frac{1/L^2}{4\pi^2 \|\vec{n}\|^2 / L^2 - z} \exp\left(\frac{2\pi i}{L} \vec{n} \cdot \vec{x}\right) / L^2 \\ &= \sum_{\vec{n} \in \mathbb{Z}^2} \frac{1}{4\pi^2 \|\vec{n}\|^2 - L^2 z} \exp\left(\frac{2\pi i}{L} \vec{n} \cdot \vec{x}\right) / L^2.\end{aligned}$$

The normalization coefficient is the square root of

$$\begin{aligned}\langle \psi_z | \psi_z \rangle &= \left\langle \sum_{\vec{n} \in \mathbb{Z}^2} \frac{\overline{\varphi_{\vec{n}}(\vec{0})}}{\lambda_{\vec{n}} - z} \varphi_{\vec{n}} \left| \sum_{\vec{m} \in \mathbb{Z}^2} \frac{\overline{\varphi_{\vec{m}}(\vec{0})}}{\lambda_{\vec{m}} - z} \varphi_{\vec{m}} \right. \right\rangle \\ &= \sum_{\vec{n}, \vec{m} \in \mathbb{Z}^2} \frac{1/L^4}{(\lambda_{\vec{n}} - z)(\lambda_{\vec{m}} - z)} \delta_{\vec{n}, \vec{m}} \\ &= \sum_{\vec{n} \in \mathbb{Z}^2} \frac{1/L^4}{(\lambda_{\vec{n}} - z)^2} \\ &= \frac{1}{L^4} \sum_{\vec{n} \in \mathbb{Z}^2} \frac{1}{(4\pi^2 \|\vec{n}\|^2 / L^2 - z)^2} \\ &= \sum_{\vec{n} \in \mathbb{Z}^2} \frac{1}{(4\pi^2 \|\vec{n}\|^2 - L^2 z)^2}\end{aligned}$$

Having found the eigenvalues and eigenfunctions of  $-\Delta_\eta$ , we've solved the

system: given the initial state

$$\psi(\vec{x}, t = 0) = \sum_0^\infty \langle \psi_j | \psi \rangle \psi_j(\vec{x}),$$

at time  $t$  the system will be in the state

$$\psi(\vec{x}, t) = \sum_0^\infty \langle \psi_j | \psi \rangle \psi_j(\vec{x}) e^{-iE_j t}.$$

To find  $p_\epsilon(t)$ , we integrate the square modulus of  $\psi(\vec{x}, t)$  over  $N(\vec{0}, \epsilon)$ . We now define what  $N(\vec{0}, \epsilon)$  is for search on the torus: let it be  $[-\epsilon, \epsilon] \times [-\epsilon, \epsilon]$ , a square  $\epsilon$ -neighborhood centered at  $\vec{0}$  (which wraps around, due to the periodic boundary conditions).

Writing  $\psi(\vec{x}, t) = \sum_j c_j \psi_j(\vec{x}) e^{-iE_j t}$ , we have

$$|\psi(\vec{x}, t)|^2 = \sum_j c_j \psi_j(\vec{x}) e^{-iE_j t} \overline{\sum_l c_l \psi_l(\vec{x}) e^{-iE_l t}} = \sum_j c_j \bar{c}_l \psi_j(\vec{x}) \bar{\psi}_l(\vec{x}) e^{-i(E_j - E_l)t},$$

and thus

$$p_\epsilon(t) = \sum_j c_j \bar{c}_l e^{-i(E_j - E_l)t} \int_{N(\vec{0}, \epsilon)} \psi_j(\vec{x}) \bar{\psi}_l(x) d\vec{x}.$$

## 4.4 Check Phase

For the check phase, we need to solve two systems: a particle in a square, and a particle in a square with a potential located at an arbitrary location. We wish to understand the difference between the energy gaps of the two systems, as this controls the detuning, which affects the distinguishability of the two systems.

The former is well-known to have solutions which are products of sines in  $x$  and  $y$  completing an integer multiple of half periods. More precisely, the

eigenfunctions of the Schrödinger equation on the interval  $[0, L]^2$  are given by  $\varphi_{\vec{n}}(x, y) = \frac{2}{L} \sin\left(\frac{n_x \pi}{L} x\right) \sin\left(\frac{n_y \pi}{L} y\right)$ , for  $\vec{n} \in \mathbb{Z}^+ \times \mathbb{Z}^+$ ; the eigenvalue of  $\varphi_{\vec{n}}$  is  $\frac{\pi^2}{L^2} \|\vec{n}\|^2$ .

If the square were shifted, then the solutions would be shifted by the same amount.

The ground state is  $\varphi_{(1,1)}$ . There are two “first” excited states:  $\varphi_{(2,1)}$  and  $\varphi_{(1,2)}$  – recall that we will orient the driving field so that only one of the two states is coupled to it. Let us decide now that  $\varphi_{(2,1)}$  is the one that is coupled to the field. The energy levels are given by  $E_{\vec{n}} = \frac{\pi^2}{L^2} \|\vec{n}\|^2$ , and so the energy gap is  $\Delta E_n = 3 \frac{\pi^2}{L^2}$ , just as in the case of the circle. Thus, the unperturbed Hamiltonian is

$$H_0 = \begin{pmatrix} 0 & 0 \\ 0 & E_e - E_g \end{pmatrix} = \begin{pmatrix} 0 & 0 \\ 0 & \Delta E_n \end{pmatrix} = \begin{pmatrix} 0 & 0 \\ 0 & 3 \frac{\pi^2}{L^2} \end{pmatrix}.$$

The driving term of the Hamiltonian has a

$$d_n = \langle g_n | X | e_n \rangle = \langle \varphi_{(1,1)} | X | \varphi_{(2,1)} \rangle$$

in it, which can easily be calculated to be  $\frac{16L}{9\pi^2}$  – again, same as for the circle.

Therefore, we have

$$H_{int}(t) = \begin{pmatrix} 0 & \frac{16L}{9\pi^2} A \cos \omega t \\ \frac{16L}{9\pi^2} A \cos \omega t & 0 \end{pmatrix}.$$

We can now write  $p_1(t)$ , the probability of finding the particle to be in state  $|e\rangle$  during a Rabi measurement. Recall, we have

$$p_1 = p_1(t_c) = \sin^2\left(\frac{\Omega_{R,n}}{2} t_c\right) = \sin^2\left(\frac{d_n A}{2} t_c\right),$$

so  $p_1(t_c) = \sin^2\left(\frac{16A}{18\pi^2} L t_c\right)$ . The  $L$  in the numerator means that as  $\epsilon$  shrinks, keeping

$p_1$  constant requires waiting proportionally longer until the first time  $p_1(t)$  hits that value.

This was all for the particle in a square box system with no potential. We move on to the next case, when the potential is present.

Now we wish to find (the two lowest energy) eigenpairs of the Schrödinger equation on  $[0, L]^2$  with a delta potential at an arbitrary point  $\vec{w}$ . The eigenpairs for this system are as described earlier this chapter: they come in two types, perturbed and unperturbed.

The unperturbed eigenfunctions are simply linear combinations vanishing at  $\vec{w}$  of the  $\varphi_{\vec{n}}$  that correspond to the same  $\lambda \in \sigma(-\Delta)$ . This means either  $\lambda$  has multiplicity greater than one, or the linear combination is degenerate and  $\lambda_{\vec{n}}$  has an eigenfunction with  $\varphi_{\vec{n}}(\vec{w}) = 0$ .

The perturbed eigenvalues  $z$  solve the quantization condition

$$\begin{aligned} \eta &= \sum_{\vec{n} \in \mathbb{Z}^+ \times \mathbb{Z}^+} |\varphi_{\vec{n}}(\vec{w})|^2 \left( \frac{1}{\lambda_{\vec{n}} - z} - \frac{\lambda_{\vec{n}}}{\lambda_{\vec{n}}^2 + 1} \right) \\ &= \sum_{\vec{n} \in \mathbb{Z}^+ \times \mathbb{Z}^+} |\varphi_{\vec{n}}(\vec{w})|^2 \left( \frac{1}{\pi^2 \|\vec{n}\|^2 / L^2 - z} - \frac{\pi^2 \|\vec{n}\|^2 / L^2}{\pi^4 \|\vec{n}\|^4 / L^4 + 1} \right) \\ &= \sum_{\vec{n} \in \mathbb{Z}^+ \times \mathbb{Z}^+} |\varphi_{\vec{n}}(\vec{w})|^2 \left( \frac{L^2}{\pi^2 \|\vec{n}\|^2 - L^2 z} - \frac{\pi^2 \|\vec{n}\|^2 L^2}{\pi^4 \|\vec{n}\|^4 + L^4} \right). \end{aligned}$$

The corresponding unnormalized eigenfunction is

$$\begin{aligned} \psi_z &= \sum_{\vec{n} \in \mathbb{Z}^+ \times \mathbb{Z}^+} \frac{\overline{\varphi_{\vec{n}}(\vec{w})}}{\lambda_{\vec{n}} - z} \varphi_{\vec{n}} \\ &= \sum_{\vec{n} \in \mathbb{Z}^+ \times \mathbb{Z}^+} \frac{\overline{\varphi_{\vec{n}}(\vec{w})}}{\pi^2 \|\vec{n}\|^2 / L^2 - z} \varphi_{\vec{n}} \\ &= \sum_{\vec{n} \in \mathbb{Z}^+ \times \mathbb{Z}^+} \frac{L^2 \overline{\varphi_{\vec{n}}(\vec{w})}}{\pi^2 \|\vec{n}\|^2 - L^2 z} \varphi_{\vec{n}}. \end{aligned}$$



The normalization coefficient is the square root of

$$\begin{aligned}
\langle \psi_z | \psi_z \rangle &= \left\langle \sum_{\vec{n} \in \mathbb{Z}^+ \times \mathbb{Z}^+} \frac{\overline{\varphi_{\vec{n}}(\vec{w})}}{\lambda_{\vec{n}} - z} \varphi_{\vec{n}} \left| \sum_{\vec{m} \in \mathbb{Z}^+ \times \mathbb{Z}^+} \frac{\overline{\varphi_{\vec{m}}(\vec{w})}}{\lambda_{\vec{m}} - z} \varphi_{\vec{m}} \right. \right\rangle \\
&= \sum_{\vec{n}, \vec{m} \in \mathbb{Z}^+ \times \mathbb{Z}^+} \frac{|\varphi_{\vec{n}}(\vec{w})|^2}{(\lambda_{\vec{n}} - z)(\lambda_{\vec{m}} - z)} \delta_{\vec{n}, \vec{m}} \\
&= \sum_{\vec{n} \in \mathbb{Z}^+ \times \mathbb{Z}^+} \frac{|\varphi_{\vec{n}}(\vec{w})|^2}{(\lambda_{\vec{n}} - z)^2} \\
&= \sum_{\vec{n} \in \mathbb{Z}^+ \times \mathbb{Z}^+} \frac{|\varphi_{\vec{n}}(\vec{w})|^2}{(\pi^2 \|\vec{n}\|^2 / L^2 - z)^2} \\
&= \sum_{\vec{n} \in \mathbb{Z}^+ \times \mathbb{Z}^+} \frac{L^2 |\varphi_{\vec{n}}(\vec{w})|^2}{(\pi^2 \|\vec{n}\|^2 - L^2 z)^2}.
\end{aligned}$$

Since we're interested in the first two energy levels, let's consider the first few eigenvalues of  $-\Delta$ . They correspond to  $\vec{n} = (1, 1), (2, 1), (1, 2), (2, 2)$ . Thus  $2\frac{\pi^2}{L^2}, 5\frac{\pi^2}{L^2}, 5\frac{\pi^2}{L^2}, 8\frac{\pi^2}{L^2}$  are the first four eigenvalues, and we have  $z_1 < 2\frac{\pi^2}{L^2} < z_2 < 5\frac{\pi^2}{L^2} \leq z_3 \leq 5\frac{\pi^2}{L^2}$ . Thus the two energy levels we care about are both perturbed eigenvalues coming from the quantization condition.

We note that if  $\eta < F(0)$ , then the ground energy is negative; as it was for  $S^1$ , the ground energy of the system may or may not be negative, depending on the value of the tuneable parameter.

To compute the detuning  $\Delta$  and  $p_2(t)$ , we need to compute  $\Delta E_p$  and  $d_p$ . Computing  $\Delta E_p$  isn't possible, as it requires finding the energy levels, which means solving a transcendental equation. We can express  $d_p$  as an infinite sum, which may not seem too useful at first. However, it will turn out that what we actually need (just like for the circle) is how these quantities scale with  $L$ . We can in fact work that out; we do so in the next section.

## 4.5 Analytic Results

We show that with the same choices of the various parameters as for search on  $S^1$ , it's possible to work out how the expected cost of the algorithm will scale as  $\epsilon$  goes to 0. As before, this isn't necessarily the optimal choice of parameters, and hence this result is about the Big O scaling of the cost, not the Big Theta scaling – that is, this is merely an upper bound on the scaling. The proofs are very similar to those from the previous chapter.

**Proposition 4.5.1.** *There is a choice of parameters so that  $p_\epsilon$  scales as  $c\epsilon^2 + o(\epsilon^2)$  as  $\epsilon$  goes to 0.*

*Proof.* If we let  $t_s = 0$ , the initial probability distribution is uniform on the space, and  $p_\epsilon$  is simply  $4\epsilon^2 / \text{vol}(M)$ . □

Using that result, we can find the scaling of  $\alpha$ , the Type I and Type II error rates of the statistical analysis during the check phase. Note that we now consider the cost a function of  $N = 1/\epsilon^2$  – how the number of epsilon neighborhoods in a torus of fixed volume scales.

**Proposition 4.5.2.** *If  $p_\epsilon$  scales as above, then  $-\ln(\alpha)$ , the numerator of  $n = -\frac{2\ln(\alpha)}{\Delta p^2}$  (the number of checks necessary in order to achieve error rate  $\alpha$ ), will scale as  $\ln(c\frac{1}{\epsilon^2}) = \ln(cN)$ .*

*Proof.* We have

$$\begin{aligned}\alpha &= 1 - \frac{1 - \delta}{p_\epsilon + (1 - p_\epsilon)(1 - \delta)} \\ &= \frac{p_\epsilon \delta}{p_\epsilon \delta + (1 - \delta)} \\ &= \frac{1}{1 + (1 - \delta)/p_\epsilon \delta} = \frac{1}{1 + \frac{\delta'}{p_\epsilon}},\end{aligned}$$

where  $\delta' = (1 - \delta)/\delta$ . Then  $\ln(\alpha) = \ln\left(\frac{1}{1 + \delta'/p_\epsilon}\right) = -\ln(1 + \delta'/p_\epsilon)$ . If  $p_\epsilon$  scales as  $c\epsilon^2 + o(\epsilon^4)$ , then  $-\ln(\alpha)$  scales as

$$\ln\left(\frac{\delta'}{c\epsilon^2 + g(\epsilon)}\right) = \ln(\delta') - \ln(c\epsilon^2 + g(\epsilon)),$$

where  $g(\epsilon)$  is  $o(\epsilon)$  by the previous result. That means

$$\begin{aligned}\ln(\delta') - \ln(c\epsilon^2 + g(\epsilon)) &= \ln(\delta') - \ln(\epsilon^2(c + \tilde{g}(\epsilon))) \\ &= \ln(\delta') - \ln(\epsilon^2) - \ln(c + \tilde{g}(\epsilon)) \\ &= \ln\left(\frac{\delta'}{\epsilon^2}\right) + \ln\left(\frac{1}{c + \tilde{g}(\epsilon)}\right),\end{aligned}$$

where the second term is bounded above by  $\ln(1/c)$ , since  $\tilde{g}(\epsilon)$  goes to 0. Therefore  $-\ln(\alpha)$  will scale as  $\ln\left(\frac{\delta'}{\epsilon^2}\right) = \ln(\delta'N)$ .  $\square$

Now we turn to  $\Delta p^2$ .

**Proposition 4.5.3.** *There is a choice of parameters so that  $\Delta p$  (which is in the denominator of  $n = -\frac{2\ln(\alpha)}{\Delta p^2}$ ) is bounded away from 0 as  $\epsilon$  goes to 0.*

Note this result implies the growth in the expected cost due to  $n$  will be due solely to  $\ln(\alpha)$ .

We will require two results for the proof of the proposition.

First, a fact: suppose  $z$  is an eigenvalue of  $-\Delta_{\eta, \vec{w}}$  on  $[0, L]^2$ . Then  $z^2/c^2$  is an eigenvalue of  $-\Delta_{\eta', c\vec{w}}$  on  $[0, cL]^2$ , where

$$\eta' = \eta - \sum_n \left( \frac{\lambda_n^2}{\lambda_n^2 + 1} - \frac{\lambda_n^2}{\lambda_n^2 + 1/c^4} \right).$$

This is easily checked by plugging into the quantization condition. The upshot is the eigenvalues of  $-\Delta_\eta$  scale like  $1/L^2$ .

Next, we have:

**Lemma 4.5.4.**  $d_p = \langle \psi_g | X | \psi_e \rangle$  scales like  $L$ , where  $\psi_g, \psi_e$  are the normalized ground and first excited states of  $-\Delta_\eta$ .

*Proof.* Recall the unnormalized eigenfunctions are of the form

$$\psi_z = \sum_{\vec{n} \in \mathbb{Z}^+ \times \mathbb{Z}^+} \frac{\overline{\varphi_{\vec{n}}(\vec{w})}}{\lambda_{\vec{n}} - z} \varphi_{\vec{n}}.$$

Thus, we have

$$d_p = \langle \psi_g | X | \psi_e \rangle = \frac{1}{\|\psi_g\| \|\psi_e\|} \sum_{\vec{n}, \vec{m}} \frac{\varphi_{\vec{n}}(\vec{w}) \overline{\varphi_{\vec{m}}(\vec{w})}}{(\lambda_{\vec{n}} - g)(\lambda_{\vec{m}} - e)} \langle \varphi_{\vec{n}}(\vec{x}) | X | \varphi_{\vec{m}}(\vec{x}) \rangle.$$

Now we count up the  $L$ s that appear in the various factors.

Using a symbolic calculation program, we find that  $\langle \varphi_{\vec{n}}(\vec{x}) | X | \varphi_{\vec{m}}(\vec{x}) \rangle$  is zero except when  $m_2 = n_2$  and  $m_1, m_2$  differ in parity, in which case the result is

$$\frac{8m_1 n_1 L}{(m_1^2 - n_1^2)^2 \pi^2}.$$

The middle factor

$$\frac{\varphi_{\vec{n}}(\vec{w}) \overline{\varphi_{\vec{m}}(\vec{w})}}{(\lambda_{\vec{n}} - g)(\lambda_{\vec{m}} - e)}$$

has a  $1/L^2$  in its numerator from  $\varphi_{\vec{n}}$  and  $\varphi_{\vec{m}}$ : recall that  $\varphi_{\vec{k}} = \frac{2}{L} \sin(\frac{k_x \pi}{L} x) \sin(\frac{k_y \pi}{L} y)$ . The denominator has two factors, each of which scales like  $1/L^2$  (recall that the eigenvalues of  $-\Delta$  scale like  $L^2$ , as do those of  $-\Delta_\eta$  if  $\eta$  is properly managed). Thus, we get a factor of  $L^4$  from the denominator, which cancels with the numerator to leave a total of  $L^2$  from the middle factor.

That leaves the normalizing factors. The squared norm of  $\psi_z$  is given by

$$\langle \psi_z, \psi_z \rangle = \sum_{\vec{n}} \frac{|\varphi_{\vec{n}}(\vec{w})|^2}{(\lambda_{\vec{n}} - z)^2}.$$

The numerator contributes  $1/L^2$  and the denominator contributes  $L^4$ , so that the squared norm scales like  $L^2$ ; hence, the norm scales like  $L$ . Thus, from  $\frac{1}{\|\psi_g\| \|\psi_e\|}$ , we get a  $1/L^2$ .

Putting it all together –  $L$ ,  $1/L^2$ ,  $L^2$  – we get an overall scaling by  $L$ , proving the result.  $\square$

A quick note: we can do the same computation for the  $S^1$ . While we solved the system without the aid of self-adjoint extensions, we would have gotten the same results. However, the self-adjoint extension theory would have given us the  $L^2$  expansion of the eigenfunctions, allowing us to easily compute  $d_p$  as above, instead of relying on symbolic calculation software. We would have found that  $d_p$  scales like  $L$  for the circle, as well. This is the result referred to immediately preceding the start of Section 3.3.

Now we can prove the proposition.

*Proof.* To bound  $\Delta p^2$  from below, we can fix  $p_1$  and then show that  $p_2$  can be

bounded away from it.

Fixing  $p_1$  is easy:  $p_1(t_c) = \sin^2(\frac{16A}{18\pi^2}Lt_c)$  depends only on  $L$  and  $t_c$ . If we grow  $t_c$  to keep  $\epsilon t_c$  fixed, then  $p_1$  will remain fixed. This means that  $t_c$  will scale as  $1/\epsilon = \sqrt{N}$ . Note the difference from the case of the circle: we still have a factor of  $1/\epsilon$ , but the formula relating  $\epsilon$  to  $N$  has changed!

Recall we don't know the value of  $p_2$ ; we get a bound on it by doing the overlapping checks to get a bound on  $r$  and the detuning  $\Delta$ . To bound  $p_2$ , first we recall from (2.5) that

$$p_2(t) = \frac{(d_p A)^2}{\Omega_{R,p}^2} \sin^2\left(\frac{\Omega_{R,p} t}{2}\right) = \frac{(d_p A)^2}{\Delta^2 + (d_p A)^2} \sin^2\left(\frac{\Omega_{R,p} t}{2}\right),$$

which is clearly bounded by  $\frac{(d_p A)^2}{\Delta^2 + (d_p A)^2}$ . The lemma we just proved tells us that  $d_p$  shrinks as  $\epsilon$  does. Thus, if we can show that our lower bound on  $\Delta$  is growing, we'll have  $p_2$  shrinking as  $\epsilon$  goes to 0.

The detuning  $\Delta$  is  $\Delta E_p - \Delta E_n$ , since we set the frequency of the field,  $\omega$ , equal to  $\Delta E_n$ . Recall we have  $\Delta E_n = 3\frac{\pi^2}{L^2}$ . Furthermore, recalling the fact preceding this proof, we know that if  $\eta$  is managed properly, both the energy levels of  $\psi_g, \psi_e$  will scale precisely by  $1/L^2$ . Thus, if the relative location of the potential in the box were fixed, the energy gaps would scale precisely by  $1/L^2$ . Hence, if we scale  $r$  to keep  $r/\epsilon$  and  $R$  fixed, our lower bound on the difference of the energy gaps also scales precisely by  $1/L^2$ , so our bound on the detuning  $\Delta$  is growing. Hence,  $p_2$  tends to 0, and  $\Delta p^2$  goes to  $p_1^2$ .  $\square$

We can now derive the scaling of the cost of the algorithm, using the given

choice of scaling of the parameters.

**Theorem 4.5.5.** *There is a choice of scaling of the parameters so that  $\mathbb{E}(\text{cost}) = (t_s + nRt_c)/p_\epsilon$  is  $O(N\sqrt{N} \ln N)$ .*

*Proof.* If we combine the last three propositions, we get

$$\begin{aligned}
\mathbb{E}(\text{cost}) &= (t_s + nRt_c)/p_\epsilon \\
&= (t_s - \frac{2 \ln(\alpha)}{\Delta p^2} R \frac{t'_c}{\epsilon})/c\epsilon^2 \\
&= \frac{1}{c} N (t_s + \frac{2 \ln(\delta' N)}{\Delta p^2} R t'_c \sqrt{N}),
\end{aligned} \tag{4.1}$$

whose highest order term is  $\frac{2Rt'_c}{c\Delta p^2} N\sqrt{N} \ln(\delta' N)$ . □

# Appendix A

## Square-root Measurement in the Continuum

### A.1 Quantum State Discrimination

**Challenge.** *Suppose your friend presents you with a quantum state  $\psi$  picked from an ensemble  $\{\psi_i, p_i\}_{i=1}^n$ . She challenges you to guess which  $\psi_i$  she chose. What is your best strategy? How well can you do?*

The challenge described above is known as the problem of quantum state discrimination. In quantum state discrimination, the allowed measurements are more general than the usual projective measurements: they are known as POVMs (positive operator-valued measurements). A POVM is given by a collection of operators  $\{\Pi_i\}_i$  that are positive semi-definite and sum to the identity. When the POVM measures a system in state  $\psi_j$ , it detects or returns the value  $i$  with probability



$\langle \psi_j | \Pi_i | \psi_j \rangle$ . There are different metrics of success for a POVM; we are concerned here with minimizing the probability of detection error,  $1 - \sum_i \langle \psi_i | \Pi_i | \psi_i \rangle$ .

One of the POVMs used in quantum state discrimination is the square-root measurement (SRM). It was first introduced as the pretty good measurement (PGM) [HW94]. It's been shown that for an ensemble with geometric uniformity (that is, when there is a group acting transitively on the states of the ensemble), the SRM is optimal in the sense of minimizing the probability of detection error [EF01]. It's given by the operators  $\Pi_i = \rho^{-\frac{1}{2}} |\psi_i\rangle \langle \psi_i| \rho^{-\frac{1}{2}}$ , where  $\rho = \sum_i |\psi_i\rangle \langle \psi_i|$ .

## A.2 SRM for a Geometrically Uniform Ensemble on a Torus

In the quantum search algorithm on a manifold, our goal is to find the marked point  $w \in M$ . During the search phase of the algorithm, we initialize the system in the uniform state and let it evolve for some time  $t_s$ . At that moment, the system is in the state  $\psi_w$ , which is unknown to us, since  $w$  is unknown. Finding the marked point  $w$  is equivalent to the quantum state discrimination problem given the uniform ensemble  $\{\psi_w\}_{w \in M}$ .

Note, however, that if the marked point were some  $w'$  instead, the state of the system  $\psi_{w'}$  would be some sort of shift of  $\psi_w$  by a transformation  $S(w, w')$ . In particular, on  $S^1$ , the various states are just rotations of each other:  $\psi_{w'}(x) = \psi_w(x - (w' - w))$ . Thus they're related to each other by the action of the group

$S^1$ . Similarly, on the torus  $T^2$ , the various states are just translates of each other (modulo the torus boundary conditions), and thus they're related by the action of the group  $T^2 = S^1 \times S^1$ . That is, we have a geometrically uniform ensemble.

We now have a general problem: given a set of states on the manifold  $T^d$  generated from a single state  $\psi_0$  by the action of the group  $T^d$ , can we perform quantum state discrimination to determine with which  $\psi_w$  we are presented?

It would seem that perhaps the continuous version of the SRM might be the POVM to use in this continuous geometrically uniform problem. In fact, there are results showing the SRM is optimal in the continuous setting as well [Chi06].

The continuous SRM is given by the operators

$$\Pi_\theta = \rho^{-\frac{1}{2}} |\psi_\theta\rangle \langle \psi_\theta| \rho^{-\frac{1}{2}},$$

where  $\rho = \int |\psi_\theta\rangle \langle \psi_\theta| d\theta$ . Since we're working in a continuous setting, we have a density, rather than probabilities: when the state is  $\psi_w$ , the output of the SRM is given by a random variable  $X$  with probability density function

$$f_X(\theta) = \langle \psi_w | \Pi_\theta | \psi_w \rangle = \langle \psi_w | \rho^{-\frac{1}{2}} |\psi_\theta\rangle \langle \psi_\theta| \rho^{-\frac{1}{2}} | \psi_w \rangle = |\langle \psi_w | \rho^{-\frac{1}{2}} |\psi_\theta\rangle|^2.$$

We find a formula for the SRM density in terms of the Fourier coefficients of the state  $\psi_0$ . We will state and prove this for  $S^1$ , but the analogous statement for  $T^d$  can be proven in exactly the same way.

**Proposition A.2.1.** *Let  $\psi_0$  be a quantum state on  $S^1 = [-\frac{L}{2}, \frac{L}{2}]/\partial$ , and let  $\psi_\theta :=$*

$\psi_0(x - \theta)$ . Then the pdf describing the outcome of the SRM when in state  $\psi_w$  is

$$\langle \psi_w | \Pi_\theta | \psi_w \rangle = \frac{1}{L} + \frac{2}{L} \sum_{m>n} |a_m| |a_n| \cos \left( \frac{2\pi}{L} (m - n)(\theta - w) \right),$$

where the sum is over unordered pairs  $m, n \in \mathbb{Z}$ , and the  $a_n$  are the Fourier coefficients of

$$\psi_0 = \sum_n a_n \exp \left( i \frac{2\pi}{L} nx \right) / \sqrt{L}.$$

*Proof.* We first work out a formula for  $\rho$ . Using the Fourier expansion of  $\psi_0$ , we see that

$$\psi_\theta = \sum_n a_n \exp \left( -i \frac{2\pi}{L} n\theta \right) \exp \left( i \frac{2\pi}{L} nx \right) / \sqrt{L}.$$

Writing  $|n\rangle = \exp \left( i \frac{2\pi}{L} nx \right) / \sqrt{L}$ , we have

$$\begin{aligned} \rho &= \int \left( \sum_m a_m \exp \left( -i \frac{2\pi}{L} m\theta \right) |m\rangle \right) \left( \sum_n \bar{a}_n \exp \left( i \frac{2\pi}{L} n\theta \right) \langle n| \right) d\theta \\ &= L \sum_n |a_n|^2 |n\rangle \langle n| \\ &= L \sum_n |a_n|^2 P_n, \end{aligned} \tag{A.1}$$

where  $P_n$  is the projection onto the  $n$ th Fourier component.

We've diagonalized  $\rho$ , allowing us to raise it to the  $-\frac{1}{2}$  power (by which we mean, take the square root of the pseudoinverse):

$$\rho^{-\frac{1}{2}} = \frac{1}{\sqrt{L}} \sum_n |a_n|^{-1} P_n.$$

We begin to calculate  $|\langle \psi_w | \rho^{-\frac{1}{2}} | \psi_\theta \rangle|^2$  step by step. First,

$$\begin{aligned} \rho^{-\frac{1}{2}} \psi_\theta &= \left( \frac{1}{\sqrt{L}} \sum_n |a_n|^{-1} P_n \right) \left( \sum_m a_m \exp \left( -i \frac{2\pi}{L} m\theta \right) |m\rangle \right) \\ &= \frac{1}{\sqrt{L}} \sum_n |a_n|^{-1} a_n \exp \left( -i \frac{2\pi}{L} n\theta \right) |n\rangle. \end{aligned} \tag{A.2}$$

Now taking the inner product with  $\psi_w$ , we have

$$\begin{aligned}
\langle \psi_w | \rho^{-\frac{1}{2}} | \psi_\theta \rangle &= \langle \psi_w | \frac{1}{\sqrt{L}} \sum_n |a_n|^{-1} a_n \exp\left(-i\frac{2\pi}{L}n\theta\right) |n\rangle \\
&= \left( \sum_m \bar{a}_m \exp\left(i\frac{2\pi}{L}mw\right) \langle m| \right) \left( \frac{1}{\sqrt{L}} \sum_n |a_n|^{-1} a_n \exp\left(-i\frac{2\pi}{L}n\theta\right) |n\rangle \right) \\
&= \frac{1}{\sqrt{L}} \sum_n |a_n| \exp\left(i\frac{2\pi}{L}n(w-\theta)\right).
\end{aligned} \tag{A.3}$$

Taking the square modulus of that, we get the result:

$$\begin{aligned}
|\langle \psi_w | \rho^{-\frac{1}{2}} | \psi_\theta \rangle|^2 &= \left| \frac{1}{\sqrt{L}} \sum_n |a_n| \exp\left(i\frac{2\pi}{L}n(w-\theta)\right) \right|^2 \\
&= \frac{1}{L} + \frac{2}{L} \sum_{m>n} |a_m| |a_n| \cos\left(\frac{2\pi}{L}(m-n)(\theta-w)\right),
\end{aligned} \tag{A.4}$$

where the 1 comes from the diagonal terms giving the norm of a unit-norm state, and the cosines are from pairing up cross terms corresponding to  $(m, n)$  and  $(n, m)$ .

□

The formula for  $T^d$  is nearly identical: the  $L^{-1}$  on the outside becomes an  $L^{-d}$ , and we sum over vectors  $\vec{m}, \vec{n} \in \mathbb{Z}^d$  instead of integers  $m, n$ .

Now suppose we wish to use the SRM for quantum search; let's consider search on the circle. Let  $\psi_0(x, t)$  be the state of the system if prepared in the uniform state and evolved for time  $t$ , if the potential were located at 0. If the potential were located at  $w$  instead, then  $\psi_w(t) = \psi_0(x - w, t)$  would be the state of the system after time  $t$ . If instead of a standard position measurement, we were to perform the SRM, the probability of the result being in  $N(w, \epsilon)$  would simply be the integral of the pdf over  $N(w, \epsilon)$ .

So, for quantum search on  $S^1$ , we would have:

**Corollary A.2.2.** *If our quantum search algorithm on  $S^1$  used the SRM in place of the standard position measurement during the search phase, we would have*

$$p_\epsilon = \frac{2}{L} + \frac{4}{L} \sum_{m>n} \frac{L|a_m||a_n|}{2\pi(m-n)} \sin\left(\frac{2\pi}{L}(m-n)\epsilon\right).$$

Note  $p_\epsilon$  is actually a function of  $t$ , as the  $a_n = a_n(t)$ , the Fourier coefficients of  $\psi(x, t)$ , vary with  $t$ .

In the small  $\epsilon$  limit,  $\sin x$  tends to  $x$ , and thus  $p_\epsilon$  is approximately

$$\frac{2\epsilon}{L} \left( 1 + 2 \sum_{m>n} |a_m||a_n| \right).$$

(Note that we can do this because we may assume that for  $t$  in some bounded range, nearly all of the bandwidth of  $\psi(x, t)$  is in the coefficients  $\{a_{-N}, \dots, a_N\}$ , so  $(m-n)\epsilon$  is small for sufficiently small  $\epsilon$ .) Thus, we see that when using the SRM, maximizing the distinguishability of the translates of  $\psi$  has been reduced to maximizing the sum of the cross terms of the Fourier coefficients of  $\psi$ . Note that the limiting case of that would be when all the coefficients are equal, *i.e.*, the Dirac delta on  $S^1$ , which certainly does maximize distinguishability from its rotations.

Some rough numerical results seemed to indicate that using the SRM in place of the standard position measurement for quantum search on  $S^1$  would improve the constant of the scaling, but not affect it otherwise. Obtaining numerical results for the SRM is more computationally expensive than for the standard position measurement. We solved the particle on  $S^1$  with a delta potential by expanding in terms of a different basis (the energy eigenstates) than the Fourier basis, so

approximating  $a_n$  entails finding the  $n$ th Fourier coefficient of many energy eigenstates. That using the SRM didn't improve the scaling of search is perhaps not surprising: the SRM is optimal for quantum state discrimination, which can be used for search, but isn't the same thing.

# Bibliography

- [CG04] Andrew M. Childs and Jeffrey Goldstone. Spatial search by quantum walk. *Phys. Rev. A*, 70:022314, Aug 2004.
- [Chi06] Giulio Chiribella. *Optimal estimation of quantum signals in the presence of symmetry*. PhD thesis, Università Degli Studi Di Pavia, 2006.
- [Chi10] Andrew M. Childs. On the relationship between continuous- and discrete-time quantum walk. *Communications in Mathematical Physics*, 294(2):581–603, Mar 2010.
- [DH96] C. Dürr and P. Høyer. A Quantum Algorithm for Finding the Minimum. *eprint arXiv:quant-ph/9607014*, July 1996.
- [EF01] Y. C. Eldar and G. D. Forney. On quantum detection and the square-root measurement. *IEEE Transactions on Information Theory*, 47(3):858–872, Mar 2001.
- [FG98] Edward Farhi and Sam Gutmann. Analog analogue of a digital quantum computation. *Phys. Rev. A*, 57:2403–2406, Apr 1998.
- [Gro96] Lov K. Grover. A fast quantum mechanical algorithm for database search. In *Proceedings of the Twenty-eighth Annual ACM Symposium on Theory of Computing*, STOC '96, pages 212–219, New York, NY, USA, 1996. ACM.
- [Hal13] B.C. Hall. *Quantum Theory for Mathematicians*. Graduate Texts in Mathematics. Springer New York, 2013.
- [HW94] P. Hausladen and W. K. Wootters. A ‘Pretty Good’ Measurement for Distinguishing Quantum States. *Journal of Modern Optics*, 41:2385–2390, December 1994.
- [Lee16] Minjae Lee. Eigenvalues of Šeba billiards with localization of low-energy eigenfunctions. *Journal of Physics A: Mathematical and Theoretical*, 49(8):085204, 2016.

- [Moc07] Carlos Mochon. Hamiltonian oracles. *Phys. Rev. A*, 75:042313, Apr 2007.
- [NC11] Michael A. Nielsen and Isaac L. Chuang. *Quantum Computation and Quantum Information: 10th Anniversary Edition*. Cambridge University Press, New York, NY, USA, 10th edition, 2011.
- [RP11] Eleanor Rieffel and Wolfgang Polak. *Quantum Computing: A Gentle Introduction*. The MIT Press, 1st edition, 2011.
- [RS75] M. Reed and B. Simon. *Methods of Modern Mathematical Physics*. Number v. 2 in *Methods of Modern Mathematical Physics*. Academic Press, 1975.
- [Šeb90] Petr Šeba. Wave chaos in singular quantum billiard. *Phys. Rev. Lett.*, 64:1855–1858, Apr 1990.
- [Ste07] Daniel A. Steck. Quantum and atom optics. Available online at <http://steck.us/teaching>, 2007.
- [Won18] Thomas Wong. Personal communication, June 2018.
- [Zal97] Christof Zalka. Grover’s quantum searching algorithm is optimal. 1997.
- [Zor80] J. Zorbas. Perturbation of self-adjoint operators by Dirac distributions. *Journal of Mathematical Physics*, 21:840–847, April 1980.